Utrecht University

Master's Thesis

A new slow-roll paradigm in multifield inflation

Author:
Iñaki Urzainki

Supervisor:
Dr. Enrico Pajer

Universiteit Utrecht

A thesis submitted in fulfillment of the requirements for the degree of Master's in Theoretical Physics

June 30, 2016

"*Don't let schooling interfere with your education.*"

Mark Twain

UTRECHT UNIVERSITY

Abstract

A new slow-roll paradigm in multifield inflation

by Iñaki Urzainki

Increasing effort has been put over the past few years to understand the consequences of the presence of several scalar fields in an early inflationary phase, since theories beyond the Standard Model generically predict such scenarios. The wealth of experimental information that can be obtained from the Cosmic Microwave Background is not yet conclusive about whether cosmic inflation was driven by one or by many scalar fields. Nevertheless, multifield inflationary models produce a great diversity of features that will potentially be measurable in the foreseeable future. In this thesis we wonder about the following elemental question regarding the widely used slow-roll approximation in multifield models: what are the conditions for multifield inflation? As surprising as it might seem, that question, which could be considered as a prior to further developments, did not have a closed answer in the literature on the subject. In this work we give the correct interpretation of the slow-roll approximation in multifield models of inflation and present some interesting new phenomena that arise from this improved understanding.

Contents

Abstract **iii**

1 Lightning introduction to Cosmology **3**
1.1 Lightning introduction to Cosmology . . . 3
1.2 The Big Bang theory . . . 10
1.2.1 Successes . . . 10
1.2.2 Problems . . . 11
Horizon problem . . . 11
Flatness problem . . . 13
A small philosophic digression . . . 14
1.3 A first look at inflation . . . 14
1.3.1 A shrinking Hubble radius . . . 14
1.3.2 Equivalent conditions for inflation . . . 15
How much inflation? . . . 16
1.3.3 Single field inflation . . . 17
Slow-roll approximation . . . 19
Other models of inflation . . . 20

2 Quantum fluctuations in inflation **21**
2.1 Quantization of a massless scalar field in de Sitter . . . 21
2.2 Cosmological perturbation theory . . . 24
2.2.1 SVT decomposition . . . 25
2.2.2 Gauge freedom . . . 26
2.2.3 The curvature perturbations ζ and $\mathcal{R}$ . . . 27
Definitions and choices . . . 27
Gauge invariant expressions . . . 28
Conservation outside of the horizon . . . 29
2.3 Contact with observations . . . 30
2.3.1 Statistics . . . 30
2.3.2 Measurable quantities and numerical values . . . 31
2.3.3 Theoretical results in single field slow-roll . . . 32
Power spectrum of scalar perturbations . . . 33
Power spectrum of tensor perturbations . . . 35
Other quantities . . . 35
2.4 Multifield. δN formalism . . . 36
2.5 Summary and discussion . . . 40

3 Multifield slow-roll under suspicion **43**
3.1 Reviewing the slow-roll conditions . . . 43
3.1.1 Single field inflation . . . 43

3.1.2 A generalization to multifield inflation 44
3.1.3 Bad choices appeared in the literature 46
3.2 Covariant multifield formalism 46
3.2.1 A large class of multifield models 46
Slow-roll parameters 49
3.2.2 $P(X, \phi^I) = X + V$ 49
Slow-roll conditions 50
Potential slow-roll parameters 50
3.3 Discussion 52

4 Slow-descent toy model **53**
4.1 Introduction 53
4.2 Analytics 53
Stability analysis 54
Slow-descent regime 55
4.3 Numerics 57
4.4 Discussion 58

A Multifield slow-roll consistency relation **65**

B $\langle \cos^2 \varphi \rangle$ between two random vectors in N dimensions **67**

Acknowledgements **69**

Preamble

Was inflation driven by a single scalar field or by many of them? This is one of the most primordial questions that one can ask in the context of inflationary models. It is also the question we had in the back of our minds while working in this thesis.

There are some good reasons why one should care about multifield models of inflation. One of them is that theories that go beyond the Standard Model (those that try to explain the fundamental physics at the high energy scales at which inflation operated) such as string theories or quantum gravity theories generically predict the presence of more than one scalar field. Therefore, chances are that multiple fields were present at the time inflation happened. Moreover, current experimental data, albeit largely improved over the past few decades, is not yet accurate enough to discard any of the two classes of models. Multifield models of inflation allow for new phenomena that cannot be produced by a single field.

Soon after we began to try to answer the elemental question, we realized that it was imperative to properly understand the slow-roll approximation in multifield models of inflation. This approximation gives rise to the most popular class of paradigm to model inflation, the one that is systematically corroborated (or at least not ruled out) by experiments. Thus, understanding the multifield slow-roll approximation could as well be considered as a prior to further developments. As surprising as it might sound, we did not find any clear account in the literature on the subject.

What is more, after completing this work we can affirm that that the usual treatment of the slow-roll approximation in multifield models, which is nothing more than a naive extension of the single field one, is not general enough. This conventional approach oversaw a whole new set of models in which the background trajectory of the fields differs significantly from that of the single field case. The aim of this work is to explore this new paradigm in detail and to expound some of its most immediate consequences.

The thesis is organized as follos:

- **Chapter 1**: We give a general introduction to Cosmology, with an emphasis in the need for a primordial inflationary phase.
- **Chapter 2**: One of the most exciting predictions of inflation has to do with the small inhomogeneities observed in the Cosmic Microwave Background (CMB). In this chapter we review the basics about the study of quantum fluctuations in Cosmology.
- **Chapter 3**: We discuss the slow-roll approximation in single field models of inflation, followed up by analogous calculations for the multifield scenario. Here we present our improved understanding of the slow-roll approximation. The correct potential slow-roll parameters are computed, and a new kind of trajectory, the *slow-descent* trajectory, arises.
- **Chapter 4**: A toy model that serves as an example of the new features introduced in the previous chapter is presented.

Notation

We will use natural units throughout the thesis, i.e.,

$$c = \hbar = k_B = 1. \tag{1}$$

Except where otherwise stated, we will also take Planck's mass to be equal to one, this is,

$$M_P = 1. \tag{2}$$

The signature of the spacetime metric is the usual in Cosmology: $(-, +, +, +)$.

Commas shall be interpreted as partial derivatives: $A(x)_{,x} \equiv \frac{\partial A(x)}{\partial x}$.

There is one acronym that will keep appearing: CMB stands for Cosmic Microwave Background.

Without further ado, let us begin with the introduction to Cosmology.

Chapter 1

Lightning introduction to Cosmology

This thesis begins with a brief review of the fundamental postulates of Cosmology and how they lead to the basic ideas developed in the XX century, which make up the Big Bang model. Further on, in section 1.2 the classic criticisms to the Big Bang model are expressed and, in section 1.3, Inflation is presented as the most elegant and suitable candidate to account for those flaws. Some elements of the simplest inflationary model, the single field model, are explored as well.

1.1 Lightning introduction to Cosmology

We tend to imagine the universe as an extrapolation of what we see when we look up at the night sky – gigantic inflamed gaseous spheres and a bunch of other bright objects surrounded by dark nothingness. We know that the universe is made out of many more galaxies like ours, and the stars in our night sky are interchanged by them in our imagination. So, there we go: the universe is a very dark place with occasional gigantic inflamed gaseous galaxies popping up. Is this a good picture?

The answer is twofold: Yes. And no.

Yes: at the scales we are used to (inside our own galaxy, even when we take the nearby clusters of galaxies) it looks like that, no doubt. And no: when we zoom out enough, the universe seems to be surprisingly smooth and uniform. Figure 1.1 shows the distribution of galaxies over large scales as seen from Earth. The larger the distance, the less clumpy it gets. And this is true no matter which direction we point our telescopes into –in one word: as seen from Earth, the Universe is *isotropic* on large scales.

If the history of science has taught us anything, it is that anthropocentric views do not help us grasp the nature of the universe. There are no reasons to think that we are living in a special part of the cosmos, or that we are some kind of privileged observers in any sense. Thus, if we accept isotropy, we are lead to conclude that the universe should appear isotropic around every point, that is, *homogeneous*.

One should be skeptical about such statements, specially when the small fraction of the universe we observe every night is not homogeneous at all. But at the same time, accepting them as working hypotheses is a sensible strategy. In fact, it turns out that homogeneity of the cosmic plasma is the fundamental principle of Cosmology. And it works much better than any other picture of the universe

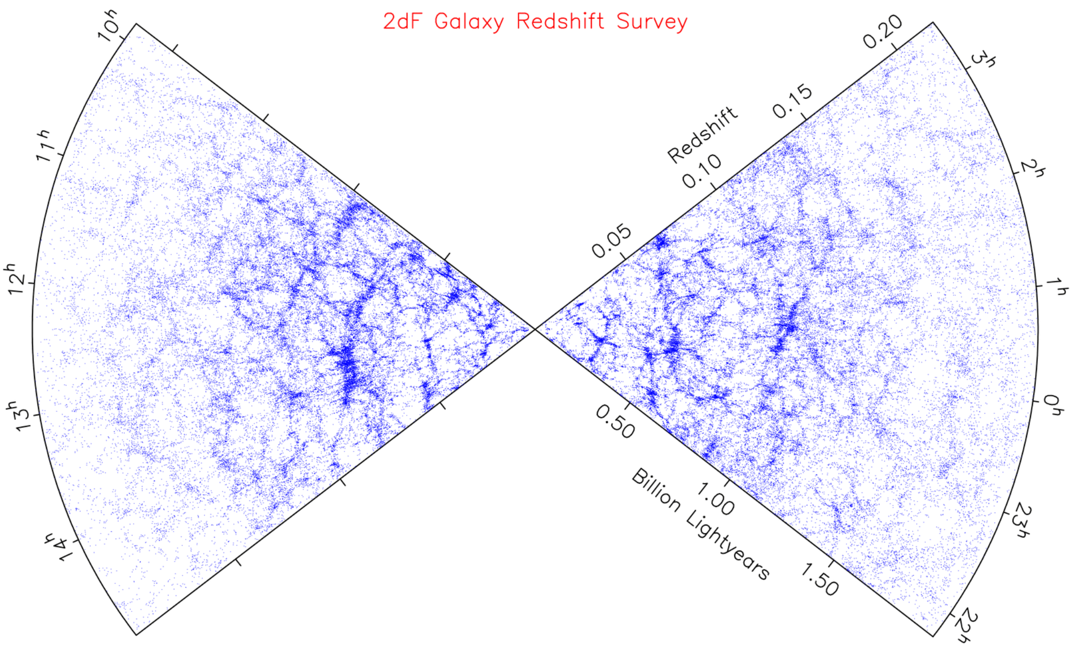

FIGURE 1.1: The distribution of galaxies tends to become uniform in large scales -or early times.

envisaged so far. Thus, let us treat it as a general truth: at large scales the universe is a homogeneous fluid.

In this section we will explore how a much sharper description of the universe arises from such a simple statement.

FLRW, a metric that describes the universe

It is already close to impossible to find a metric that describes the Earth, an imperfect sphere as it is, in full precision. What hope do we have then in finding a metric that describes the whole universe?

This apparently impossible task is greatly simplified if we adjust our strategy and look for a metric that suits the principle of homogeneity. In fact, the simple metric

$$ds^2 = -dt^2 + a^2(t)\left(\frac{dr^2}{1-\kappa r^2} + r^2\left(d\theta^2 + \sin^2\theta d\phi^2\right)\right) \tag{1.1}$$

is the most general representation of a homogeneous and isotropic universe.

Instead of using spherical coordinates, we can write the metric in terms of the *comoving coordinates* x^i,

$$ds^2 = -dt^2 + a^2(t)\gamma_{ij}dx^i dx^j, \tag{1.2}$$

where the information about the curvature is now included in the spatial metric γ_{ij}. This metric, in either of the two forms (A.1) or (A.3), is known as the **FLRW** (Friedmann-Lemaître-Robertson-Walker) metric.[1]

Its simplicity is remarkable. The ten initial independent components of the metric have been reduced, due to homogeneity, to a function of time $a(t)$ and a constant κ. Note that introducing any other term such as a g_{0i} component, or making $a(t)$ depend also on the position x^i, would break the required symmetry.

One of the consequences of homogeneity and isotropy is that the spatial hypersurfaces must have constant curvature. It is the curvature parameter κ that realizes the three possible options: $\kappa = 0$ corresponds to flat slices and $\kappa \pm 1$ to positive and negative curvature, respectively. Any other value of κ can be absorbed into the scale factor by a redefinition of r. To see this, take $\kappa \to \alpha^2\kappa$ and redefine $r' = \alpha r$. The metric then would look like

$$ds^2 = -dt^2 + \alpha^{-2}a^2(t)\left(\frac{dr'^2}{1-\kappa r'^2} + r'^2\left(d\theta^2 + \sin^2\theta d\phi^2\right)\right), \tag{1.3}$$

and we could define a new scale factor $a' = \alpha a$, thus maintaining the form of the metric given above. Latest CMB and Large Scale Structure observations[1] strongly favor a universe which is almost flat, and for the rest of this work we will set $\kappa = 0$, unless otherwise stated.

The other parameter, the *scale factor* $a(t)$, gives the relative size of the universe as a function of the cosmic time[2] t. It is customary to make the choice that the scale factor is equal to one now, i.e.,

$$a(t_{\mathrm{now}}) \equiv a_0 = 1. \tag{1.4}$$

Energy-momentum tensor and Einstein Equations

Homogeneity and isotropy also put constraints on the energy momentum tensor, requiring it to take the form of a perfect fluid,

$$T^{\mu}{}_{\nu} = \begin{pmatrix} -\rho & 0 & 0 & 0 \\ 0 & p & 0 & 0 \\ 0 & 0 & p & 0 \\ 0 & 0 & 0 & p \end{pmatrix}. \tag{1.5}$$

Its conservation equation yields

$$\nabla_\mu T^{\mu\nu} = 0 \implies \dot\rho + 3H(\rho + p) = 0, \tag{1.6}$$

where $H \equiv \frac{\dot a(t)}{a(t)}$ is the *Hubble parameter.*

[1] The FLRW metric is also called FRW, or even RW, deliberately forgetting about some great physicists that were somehow involved in its discovery.

[2] The fact that there exists a unique and general "clock" to assign time to any event seems quite a big assumption from the point of view of General Relativity. But this is again a consequence of the universe being isotropic and homogeneous throughout its history: spacetime can be partitioned into foliations of non-intersecting global hyperplanes that are orthogonal to the timelike geodesics. Since they do not intersect each other, there is one single parameter, the cosmic time, that can describe time in any of the foliations.

In this simple universe, only two of the Einstein Equations are linearly independent. They form a system of non-linear differential equations, known as *Friedmann Equations*,

$$H^2 = \frac{\rho}{3M_P^2} - \frac{\kappa}{a^2} \tag{1.7}$$

$$\frac{\ddot{a}}{a} = -\frac{\rho + 3p}{6M_P^2}, \tag{1.8}$$

where $M_P \equiv \left(\frac{\hbar c}{8\pi G}\right)^{1/2} \simeq 2.4 \cdot 10^{18} GeV$ is the reduced Planck mass, often set to one in the remainder of this work, except when specifically indicated otherwise.

Constituents of the universe

To make some progress in the description of the universe we can choose an equation of state to characterize the fluid. The perfect fluids relevant to cosmology obey the simple equation of state

$$\rho = wp, \tag{1.9}$$

where w is a time-independent constant. The continuity equation (1.6) can then be integrated to give

$$\rho \propto a^{-3(1+w)}. \tag{1.10}$$

What kind of things can be found out there? Well, there is *matter* such as the visible nuclei and electrons that make up stars and galaxies. Its pressure can be neglected and therefore $\rho_m \sim a^{-3}$. We also have to account for massless particles like photons, gravitons (if any), or highly relativistic particles like neutrinos (at least until they slow-down enough to become non-relativistic. The exact time depends on their mass, but it is around $z = 100$.). These form what is known as *radiation*, which is characterized by $w = 1/3$. Thus, in a radiation-dominated universe the energy density falls of slightly faster than in the matter-dominated case, $\rho_r \sim a^{-4}$. This goes together with the idea that, as the universe expands, photons get redshifted so that their energy density decays faster than that of matter [3].

Interestingly enough, we have recently discovered that matter and radiation are not enough to describe the evolution of the universe. The fact that the expansion of the universe is currently accelerating implies that the energy density must be dominated by a mysterious fluid, fairly enough called *dark energy*, with $w = -1$ and therefore constant energy density $\rho_\Lambda \sim a^0$. But there is even more to this. Experiments show that the amount of matter that we can observe (called *'baryonic' matter* despite the fact that some leptons are included) is not enough to account for all the matter-like energy density. For instance, astronomical objects move with a larger peculiar velocity and attract each other more violently than if there was only ordinary matter.

Measuring distances

The fact that the universe as a whole is changing its size makes measuring distances in it a bit involved. One option is to take the distance between two points (say, two galaxies) to be fixed on an imaginary

[3] For the time being, we are accepting that the universe is expanding as a general truth. We will get to the evidence that points towards such statement in section 1.2.

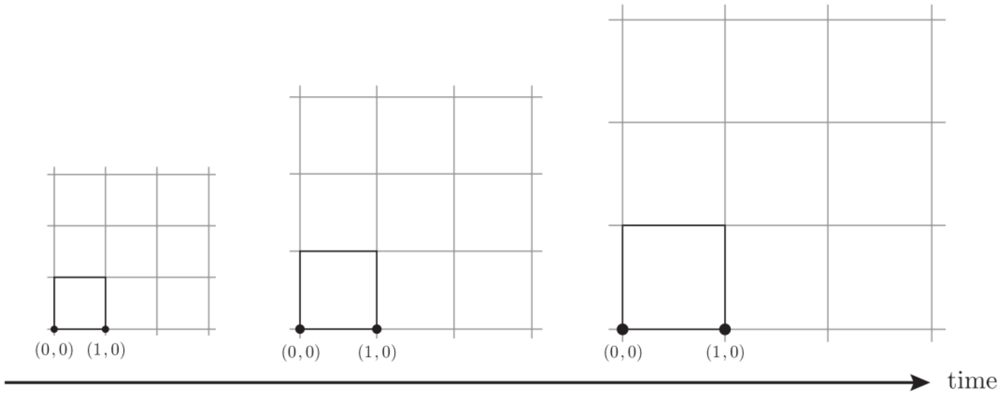

FIGURE 1.2: In this example, the comoving distance between two points of the grid is equal to 1 at any time, whereas the physical distance gets larger as time evolves. Image taken from [2].

grid, while the grid expands or contracts. In this case, the distances are measured by the recently introduced comoving coordinates x^i. Another option is to use the physical distance, defined as

$$x^i_{physical} = a(t)x^i, \tag{1.11}$$

which gets larger or shorter as time evolves. These two distances are schematically explained in Figure 1.2.

A comoving time that will be of particular interest later on is the *comoving particle horizon*, which gives the total distance a free photon could have traveled since $t = 0$. Since we have set $c = 1$, the comoving distance light travels in a time dt is $dx = dt/a$. Thus, the particle horizon is

$$\eta = \int_0^t \frac{dt'}{a(t')}. \tag{1.12}$$

The reason this distance deserves a special commentary is because regions of the universe separated a distance greater than η apart cannot be causally connected. This concept will be crucial for our discussion about the Big Bang model and inflation.

A brief history of the Universe

As the old slogan goes, *looking far away in space means looking back in time*. This makes Cosmology be, rather than the branch of science that studies the universe, the one that cares about its history.

In this section I will review what is known about what has happened in these $13.8 \cdot 10^9$ years, but also will point out the shortcomings in our understanding. We will take Table 1.1, which displays some benchmarks in the history of the universe, as our tourist guide.

But before, let us take a small digression so that we can agree on how to describe time. There are basically four ways to characterize any epoch in the history of the universe. First of all, we have the obvious cosmic time t, the proper time of comoving observers, which is very useful to realize at a qualitative level how terribly big -or small- the time scales involved are, but not as much to talk about physical processes. Second of all, we can use the value of the scale factor $a(t)$, or even more commonly, the *redshift* z, given by

$$z(t) = \frac{1}{a(t)} - 1. \tag{1.13}$$

We can also use the temperature of the cosmic fluid as an indicator. The wavelengths of the photons get redshifted as the universe expands, which makes their temperature scale as $T \sim a^{-1}$. We can use the temperature we measure now to obtain

$$T = \frac{T_0}{a(t)}, \tag{1.14}$$

where $T_0 \simeq 2.725K$.

Last but not least, we might as well talk about the energy of the fluid, given simply by $k_B T$, which is the reason why I will abuse of the language and use the two interchangeably. These energy scales are much more useful to unveil the physics behind them. As an example, the values today would be $t_0 \simeq 13.8 \cdot 10^9$ years; $a_0 = 1$ or $z_0 = 0$ (by definition); $T_0 = 2.725K$; and $k_B T_0 = 2.35 \cdot 10^{-4} eV$.

Having set the stage, we are now ready to make the leap and start from the beginning –the beginning of it all, in fact.

	Cosmic time	Energy	Redshift
Planck epoch (?)	$< 10^{-43}$ s	10^{18} GeV	
String scale (?)	$\gtrsim 10^{-43}$ s	$\lesssim 10^{18}$ GeV	
Inflation (?)	$\gtrsim 10^{-34}$ s	$\lesssim 10^{15}$ GeV	
Baryogenesis (?)	$< 10^{-10}$ s	> 1 TeV	
Electroweak unification	10^{-10} s	1 TeV	
Quark-hadron transition	10^{-4} s	150 MeV	
Dark matter freeze-out (?)	?	?	
Neutrino decoupling	1 s	1 MeV	
Electron-positron annihilation	6s	0.5 MeV	
Big Bang Nucleosynthesis (BBN)	3 min	100 keV	$\sim 10^8$
Matter-Radiation Equality	10^4 yr	1 eV	10^4
Recombination	260-380 kyr	0.26-0.33 eV	1100-1400
Photon decoupling (CMB)	380 kyr	0.23-0.28 eV	1000-1200
Reionization	100-400 Myr	2-7 meV	25-6
Galaxy formation	600 Myr	1 meV	~ 10
Dark energy-matter equality	10^9 yr	0.33 meV	0.4
Now	13.8 Gyr	0.24 meV	0

TABLE 1.1: Brief summary of the history of the Universe. The events marked with a question mark are either based on more speculative ideas, or fewer details are known about them.

The history of the universe since the first 10^{-10} seconds to today is governed by physical processes that are well known and established by experiments. But beyond that time, energy scales that have yet not been probed in particle accelerators ($\gtrsim$ 1TeV) start being relevant, and we cannot rely on the known physics anymore. This is certainly a drawback, but it can also be regarded as good news:

exploring the very beginning of the universe could shed some light on the exciting and unknown high energy physics.

Very little is known about the laws of physics around the string scale or grand unification epochs; hence the question marks in Table 1.1. The unanswered questions about inflation, on the other hand, are of a very different kind. Of course, inflation is the main topic of this Master's Thesis, and as such, it will be explained in detail in due course. For the time being, it is enough to point out that although the full details of the process are still obscure, there is a general consensus in regarding the inflationary theory as a well established fact about the history of our universe.

Some more unanswered questions surround baryogenesis. There is no reason to suppose a primordial matter/anti-matter asymmetry, but we do observe an overabundance of matter over anti-matter today. Although many ideas to predict the observed amounts of matter and anti-matter exist, none of them is singled out by experiment, and so the question remains open.

Further down the energy scale we begin stepping on solid, experimentally tested ground. Around 100GeV the electroweak symmetry is broken and the gauge bosons of the weak interactions $W^{\pm}$ and Z receive their masses through the Higgs mechanism. At temperatures below 100MeV we find ourselves at the energy scale of the strong interactions, where quarks and gluons are able to form bounded systems such as baryons and mesons. Before that, the universe is too hot to let these bounded systems come to birth; every time one baryon or meson is created, the high temperature of the plasma excites it back to the unbounded state. From here on, our arguments will follow that simple logic: particles that we observe today as bounded states will only be formed when the energy of the cosmic plasma drops below their binding energy.

Dark matter freeze-out is the next one on the list. As was already mentioned, little is known about its properties, but since it interacts with ordinary matter very weakly, we expect it to have decoupled relatively early on. For instance, the popular WIMP (Weakly Interacting Massive Particle) models explain the observed relic amount of dark matter surprisingly well, and they would freeze out around 1MeV.

It is a consequence of the electroweak phase transition that the strength of the weak interactions decrease as the temperature of the universe drops. As a result, particles that only interact with the plasma through weak interactions, the case of neutrinos, stop interacting with it at around 1MeV.

Shortly after neutrinos have decoupled from the primordial plasma, the energy drops below 500keV, allowing electrons and positrons to start annihilating each other. The energy created in such reactions is transmitted to photons, still coupled to the plasma, but not to the neutrinos.

Three minutes later, light elements (almost exclusively hydrogen and helium) are created because the energy needed to separate them is above 100keV. This process is known as Big Bang Nucleosynthesis (BBN).

We have to wait thousands of years until the next relevant event takes place. Until $\sim$ 1eV photons, electrons and protons are tightly coupled together via Compton and Coulomb scattering, and almost all hydrogen is ionized. Energetics favors the production of neutral hydrogen, that has a binding energy of $\epsilon_0 = 13.6$eV, but there are so many more photons than protons that the production of hydrogen atoms is delayed until 0.1eV. From this moment on, photons do not interact anymore with the plasma and simply free stream. This turns out to be a key process to understand modern Cosmology. We, observers that live $13.7 \cdot 10^9$ years in the future, can observe those last-scattered photons now in the night sky. Due to the massive expansion of the universe, the light has been redshifted into the microwave frequency, and hence the name of that last-scattering surface is the Cosmic Microwave Background (CMB). The great majority of improvements in Cosmology in the last few decades have come from more and more detailed observation of those ancient photons.

Our historical review might as well end up here. Being aware as we are that we forgot to comment on some important events such as reionization or galaxy formation, we hope that the reader has gained by now a general understanding of the context in which this thesis is set.

Before finishing, there were two items of the table that went unnoticed so far on which I would like to comment now: the epochs of matter-radiation and matter-dark energy equality. Before $1eV$ most of the constituents of the universe behaved as the radiation mentioned earlier, so that the total energy density was dominated by radiation, i.e., $\rho \simeq \rho_r \sim a^{-4}$. Around 1eV non-relativistic matter starts playing an important role and $\rho_m \approx \rho_r$. From that moment on and until a very short –in the cosmological sense– time ago, the universe was dominated by matter. But at an energy of around $0.33MeV$, the energy density of the universe began to be dominated by the mysterious dark energy.

Satisfactory, isn't it? We seem to know a lot of stuff about how we got here. But beware! Don't count the chickens before they're hatched. It is the aim of the following sections to explain why this is an incomplete and rather problematic view of the history of our universe –as well as to give an elegant solution.

1.2 The Big Bang theory

Besides being a popular sitcom where a theoretical physicist is the main character, the Big Bang theory is also the name given to an equally popular scientific theory developed in the XX century. In the following sections we will go over the main ideas, and also find out why it does not work. But before criticizing it for the flaws it might have, let us take a minute to admire what it got right.

1.2.1 Successes

The birth of the Big Bang theory is usually related to an experimental discovery by Hubble in 1929. He found out that galaxies are receding away from us at a speed proportional to their distance, that is,

$$v = H_0 x_{phys}, \tag{1.15}$$

where x_{phys} is the physical distance the galaxy is at, and H_0 is the Hubble parameter at the time of the observation. The original plot that appeared in the historic article [3] is shown in Figure 1.3. This observation is corroborated by modern experiments.

It was a decisive discovery in the way we understand the evolution of our universe because it taught us two important things. First of all, that the universe is expanding; it is not static. Second, that if objects are receding away from us and we play the film backwards, then we should see how the universe shrinks. Thus, the universe should have been denser and therefore hotter in the past.[4]

These ideas can be regarded as the starting point of a cosmological model that has the power to explain all of what we discussed in the previous sections. In sum, it successfully explicates for the expansion of the universe understood as a homogeneous fluid, it can explain the abundance of light

[4]These ideas were not easy to swallow: the expanding view of the universe was not accepted until the seventies, when the CMB was measured for the first time.

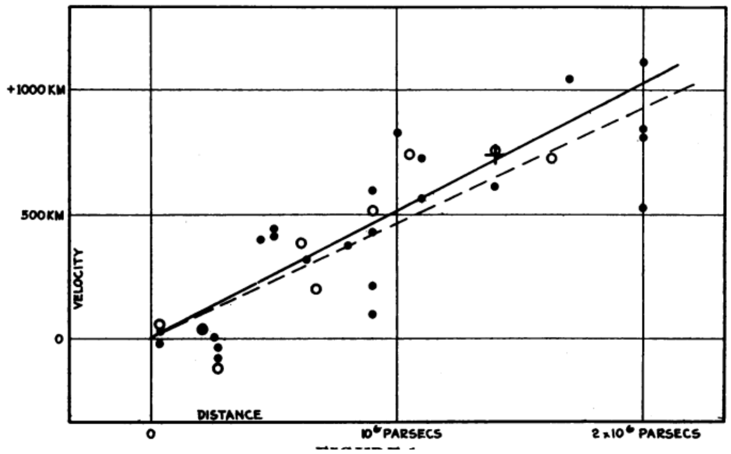

FIGURE 1.3: Hubble's discovery: the velocity at which distant objects recede from us is proportional to their distance. Taken from [3].

elements and can account for the formation of structure. There were not many questions that escaped from being answered by this model.

However, another experiment carried out in 1965, this time by Penzias and Wilson [4], was about to change things[5]. Almost unintentionally, they discovered and measured the radiation coming from the CMB. What they saw is simulated in Figure 1.4. No matter where they pointed their telescopes into, the measurement was the same: a constant background noise. The homogeneity of the CMB has been corroborated by more precise measurements, the last of which [1] took a beautiful picture of the CMB shown in Figure 1.5.

Actually, to some extent, this was a great success of the predictive power of the Big Bang model. Dicke, Peebles and Wilkinson, from Princeton, had already concluded, before the experiment, that such a microwave background is a direct consequence of the massive energy blast of the Big Bang. However, it also hid a more deep and problematic puzzle. The tremendous uniformity of the radiation made themselves wonder: why is the CMB so homogeneous?

1.2.2 Problems

To understand why the question posed above is pointing at a flaw of the Big Bang model, we will discuss two problems related to the homogeneous initial conditions.

Horizon problem

First of all, let us analyze the question we want to answer. The universe today, $13.7 \cdot 10^9$ years after the last scattering, is quite homogeneous. And inhomogeneities are gravitationally unstable, growing in time –denser regions of space attract more matter. Therefore, the universe in the time of the CMB should have been extremely homogeneous. In principle there is nothing wrong with that.

The worries arise when we learn that images like the one shown in Figure 1.4 encompass a large number of causally disconnected regions of space. This means that photons in two separated parts of

[5] The history behind the discovery is certainly worth a look. For instance, the book *3K:The Cosmic Microwave Background Radiation* by R.B.Partridge covers it.

the CMB could not possibly interact, and therefore it is surprising how they *knew* that they should thermalize with each other. Let us put this in more precise terms. We begin by taking the comoving particle horizon defined in eq.(1.12) and writing it in the following way

$$\eta = \int_{\ln(a_i)}^{\ln(a)} d\ln a' (a'H)^{-1}, \tag{1.16}$$

where by the subscript i we mean the initial value, at $t = 0$. We interpreted it as the total length light has traveled since the beginning of the universe. Therefore, we argued, objects that are further apart than η could never have communicated.

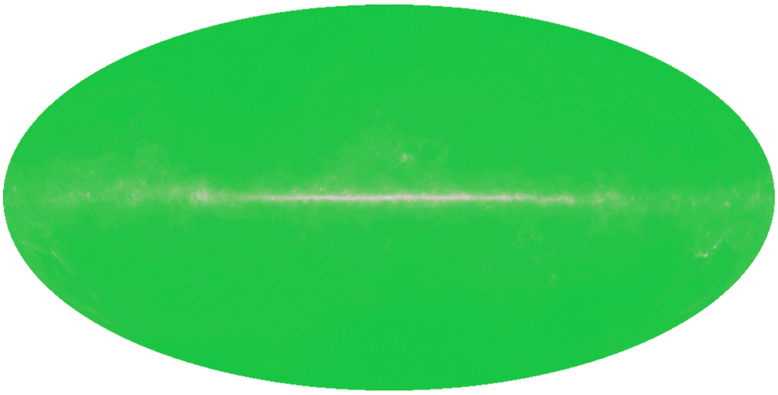

FIGURE 1.4: A view of the sky as would have been seen by the microwave receiver of Penzias and Wilson, if it could have surveyed the whole sky. The white blurred line is due to the radiation of our own galaxy. It is a simulated image taken from http://wmap.gsfc.nasa.gov/, the official NASA web page of the WMAP mission.

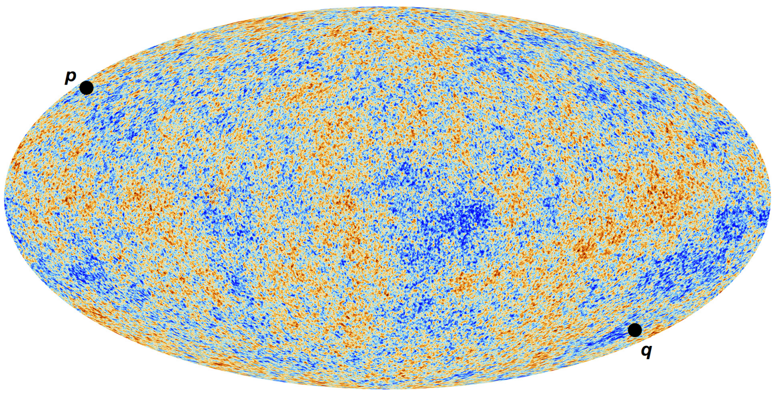

FIGURE 1.5: Last image of the CMB, as got by the Planck satellite in 2015. Despite the heterogeneous appearance, the difference in temperature between the differently colors is around $10^{-5}K$. Perhaps, the most perfect blackbody spectrum known to date. (Radiation coming from our own galaxy has been removed). Image taken from http://planck.cf.ac.uk/science/cmb.

To make the following point clearer, it is useful to introduce another comoving distance with a similar interpretation. $(aH)^{-1}$ is called the *Hubble radius*, and it is the distance that photons can travel within one Hubble time. Therefore, if two particles are further apart than $(aH)^{-1}$, then they cannot talk to each other *now*.

Combining the Friedmann equation (1.7) with eq. (1.10) we get

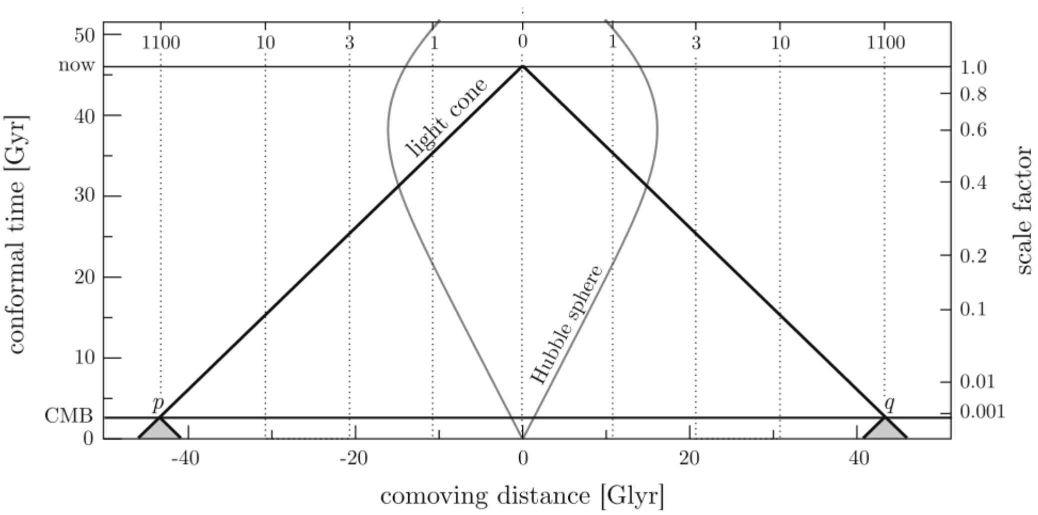

FIGURE 1.6: The horizon problem in the Big Bang model. p and q are two points in opposite directions in the CMB. There is not enough time for their past light cones to intersect, and therefore they were not in causal contact. The same applies to any two points that are separated by more than 1 degree on the sky. Picture taken from [2]

$$(aH)^{-1} = \frac{1}{H_0} a^{\frac{1+3w}{2}}. \tag{1.17}$$

All common sources of energy (except dark energy, but that only dominates at the very end) satisfy the Strong Energy Condition, i.e., $1 + 3w > 0$, and so it is quite reasonable to assume that the Hubble radius increases monotonically as the universe expands. Thus, the integral in eq. (1.16) will be dominated by the latest contribution. Indeed, in the limit $t \to 0$ we have that $a_i \to 0$ and we get, at any time t

$$\eta = \frac{2}{1+3w}(aH)^{-1}. \tag{1.18}$$

So, the comoving particle horizon is proportional to the Hubble radius, and thus it increases as the universe expands. This automatically implies that regions of the universe that are beginning to be in causal contact now were not able to communicate in the past. In particular, there is no way in which photons from the last scattering that we observe today in the CMB could have reached thermal equilibrium. Figure 1.6 shows this problem schematically.

In fact, just to mention some numbers, the CMB is made up of about 10^4 causally disconnected patches. Yet observations say that the CMB is an almost perfect blackbody spectrum, with a relative difference in temperature of $\mathcal{O}(10^{-4})$K. This is known as the *Horizon problem*.

Flatness problem

It is somewhat confusing *per se* that our universe is very close to being exactly flat now. Given that matter affects curvature and that the universe is such a "dynamic" place, it seems too big a coincidence. But this issue gets thornier early on.

Looking again at the Friedmann equation (1.7) and defining a critical density $\rho_{crit} \equiv 3H^2$, we see that

$$\left|1-\frac{\rho}{\rho_{crit}}\right| = \frac{\kappa}{(aH)^2}. \tag{1.19}$$

Here too, as we saw in the preceding section, the Hubble radius $(aH)^{-1}$ increases with time. But then this means that $\left|1-\frac{\rho}{\rho_{crit}}\right|$ must diverge with time, or, in other words, the universe must have been much flatter in the distant past. Putting some numbers into the mix, the amount of homogeneity we measure today implies that at the time of the BBN the left hand side must have been of $\mathcal{O}(10^{-16})$.

This extremely fine tuning at the beginning of the universe is hard to swallow. It somehow implies that all massive objects had just the right amount of initial velocity: if they had been slower, the universe would have recollapsed very quickly, while if they had been too fast, the universe would have expanded too much and would have become almost empty. This is what we call the *flatness problem*.

A small philosophic digression

It is worth pointing out that the horizon and flatness problems are not, strictly speaking, faults of the theory. The Big Bang model is able to predict the flatness we observe today, and even the very homogeneous CMB. The only caveat is that in order to do so it needs a really precise and fine-tuned set of initial conditions. In fact, the underlaying question is profound: should we consider the initial conditions as part of a physical theory? For instance, Maxwell's equations do not give us any information about what the initial state is; they rather let us evolve a given set of initial conditions.

But still, needing fine-tuned values for the beginning of our universe is somewhat disappointing. The reason might be that we have been brought up being skeptical about improbable accidents –especially when that accident results in our universe and ourselves.

No need to worry too much, though. Inflation is an elegant mechanism that explains the homogeneity from a quite general set of initial conditions. The skeptical reader will sigh in relief.

1.3 A first look at inflation

An early stage of inflation was first proposed by Starobinsky [5] and Guth [6]. These first attempts explained that inflation could solve the horizon and flatness problem, but the specific models were sligtly problematic. Shortly afterwards, slow-roll inflation was proposed independently by Linde[7] and by Albrecht and Steinhardt[8].

These two ideas, namely how inflation fixes the problems of the Big Bang theory and what slow-roll inflation is, will be presented in this section. Once they have been introduced, we will have covered, albeit rather superficially, most of what is known as the ΛCDM model, the Standard Model of Cosmology.

1.3.1 A shrinking Hubble radius

As promised, we are about to give the beautiful idea that cures the weaknesses of the Big Bang model. The title of this section says it all: let us postulate an initial epoch where the Hubble radius shrank. Still not convinced? Let me rephrase it a bit: Particles that do not communicate today were inside the comoving particle horizon long ago, and thus in causal contact.

To see why we need an era of shrinking Hubble radius to account for such a behavior, let us look at eq. (1.16) again. It is possible that η is larger than $(aH)^{-1}$ now, so that particles that are not in causal contact today were in the past. In order to achieve this we need that $(aH)^{-1}$ was once bigger than it is now, so that η got most of its contribution from early times.

Such a situation is depicted in Figure 1.7. It should be said that what we called the initial singularity at $t = 0$ is not a singularity anymore; it just indicates the transition point between an inflationary era and the standard Big Bang evolution.

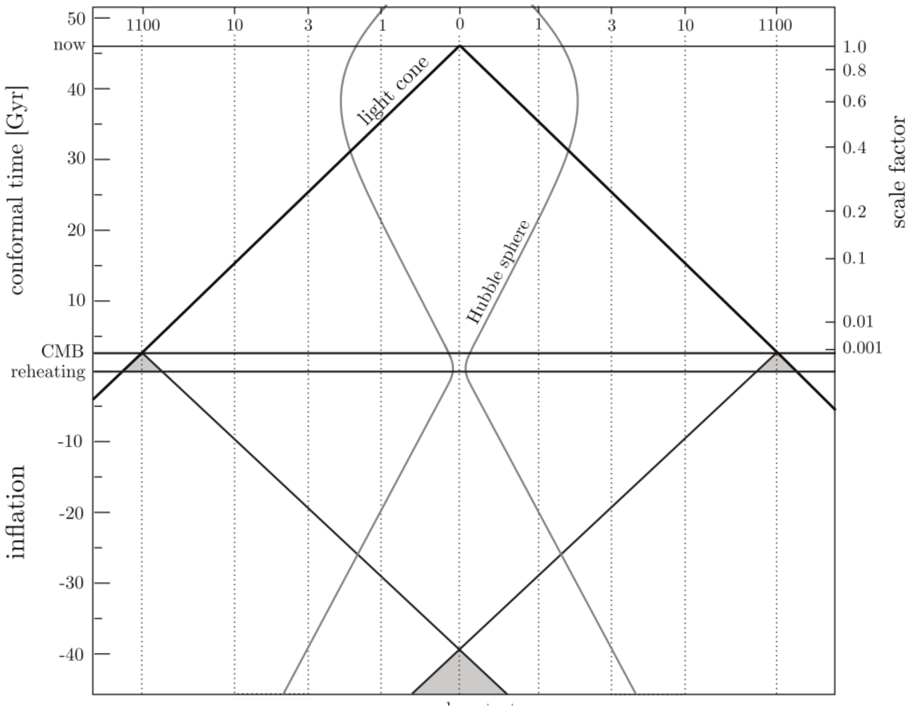

FIGURE 1.7: Inflationary solution to the horizon problem. The comoving Hubble radius (called “sphere” here) shrinks during inflation. All points in the CMB were in causal contact at some point. Picture taken from [2]

So we have solved the Horizon problem! Now the homogeneity of the CMB is a natural consequence: temperature is uniform because distant photons did interact in the past and could reach equilibrium.

What about the Flatness problem? Well, let us look again at eq.(1.19). If the Hubble radius $(aH)^{-1}$ shrinks, then inflation drives the universe toward flatness; independently of what the fraction ρ/ρ_{crit} was before inflation, it will be very close to zero after it. Second problem solved, then.

Let us examine this idea of the shrinking Hubble radius more mathematically and see what specific conditions are needed for it.

1.3.2 Equivalent conditions for inflation

A decreasing Hubble radius means that

$$\frac{d}{dt}\left(\frac{1}{aH}\right) < 0. \tag{1.20}$$

Manipulating this expression we see

$$\frac{d}{dt}\left(\frac{1}{aH}\right) = \frac{d}{dt}(\dot{a}^{-1}) = -\frac{\ddot{a}}{\dot{a}^2} < 0, \tag{1.21}$$

and, therefore

$$\ddot{a} > 0 \tag{1.22}$$

gives an inflationary solution. Inflation is indeed an epoch of accelerated expansion.

Another way of looking the same calculation is in terms of H

$$\frac{d}{dt}\left(\frac{1}{aH}\right) = \frac{d}{dt}(\dot{a}^{-1}) = \frac{1}{a}\left(\epsilon - 1\right) < 0, \tag{1.23}$$

where we have defined ϵ to be

$$\epsilon \equiv -\frac{\dot{H}}{H^2}. \tag{1.24}$$

Thus, inflation exists if and only if

$$\epsilon < 1. \tag{1.25}$$

This explains the other name given to inflation: *the quasi-de Sitter expansion*. The purely de Sitter limit is $\epsilon \to 0$, i.e., $H =$ constant.

What kind of fluid does support inflation? Take a look at eq. (1.8). As $a(t)$ is always positive, an inflationary regime with $\ddot{a} > 0$ requires $-(\rho + 3p) > 0$, i.e.,

$$p < \frac{-\rho}{3}. \tag{1.26}$$

But this is a rather strange fluid because a) it violates the SEC mentioned above and b) its pressure is negative. As we will see in section 1.3.3, these conditions are quite easy to fulfill in a physical theory.

How much inflation?

We have repeatedly said that we appear to live in a homogeneous universe. If inflation is to solve the Horizon problem, then it should explain the uniformity on temperature of the most distant points we are able to see today. True, probably the universe is homogeneous at even larger scales, but without further speculations we can only set a lower bound on the amount of time inflation should have lasted. So, in order to solve the Horizon problem we need that, at the very least, the observable universe today fits in the Hubble radius at the beginning of inflation, i.e.,

$$\left(a_0 H_0\right)^{-1} < \left(a_I H_I\right)^{-1}, \tag{1.27}$$

where the subscript I stands for the beginning of inflation.

The ratio in temperature (or energy) since inflation ended until today is

$$\frac{T_0}{T_e} \simeq 10^{-28}, \tag{1.28}$$

where the subscript e labels the end of inflation.[6]

Now, in order to simplify the calculations, let us suppose that after inflation the universe has been always dominated by radiation. This is a crude approximation since, as we have seen, there have also been epoch dominated by matter or by dark energy, in which the universe evolved differently. However, it turns out that this computation gives a pretty good estimation of the time inflation needed to last. As we saw earlier in this introduction, during radiation era we have that $H \equiv \frac{\dot{a}}{a} \propto a^{-2}$. This allows us to relate the Hubble radius to the ratio of temperature of eq. (1.28) quite easily:

$$\frac{T_0}{T_e} = \frac{a_e}{a_0} = \frac{a_0 H_0}{a_e H_e}. \tag{1.29}$$

Combining equations (1.27) and (1.29) we see that

$$(a_I H_I)^{-1} \gtrsim 10^{28} (a_e H_e)^{-1}. \tag{1.30}$$

Hence, to be able to explain the horizon and flatness problems, the Hubble radius during inflation had to shrink about 10^{28} times. Furthermore, supposing a purely de Sitter inflation, that is, $\epsilon = 0$ or $H = \text{const.}$, we get that

$$\frac{a_e}{a_I} \gtrsim 10^{28}. \tag{1.31}$$

These huge numbers makes us favor logarithmic scales. The *number of efolds* N are defined as follows:

$$dN \equiv \pm H dt, \quad \text{or} \quad N_e - N_I \equiv \pm \ln\left(\frac{a_e}{a_I}\right) \tag{1.32}$$

where the plus and minus signs refer to two different conventions: either the number of efolds increases (plus) or decreases (minus) as time goes on.

With this definition, we get that the number of efolds that inflation should have lasted is

$$\ln\left(\frac{a_e}{a_I}\right) = |N_e - N_I| \gtrsim 64. \tag{1.33}$$

1.3.3 Single field inflation

Single field inflation is a really simple physical model that can account for a inflationary regime. It is worth noting that, as simple as it might be, it is not yet ruled out by experiments –to some extent, it is even favored by them.

The model consists of a scalar field $\phi(t)$, called the *inflaton*, which is minimally coupled to gravity. The action, therefore, should be the sum of the Einstein-Hilbert action and the action for a scalar field with a canonical kinetic term:

$$S = \int d^4x \sqrt{-g} \left[\frac{R}{2} + \frac{1}{2} g^{\mu\nu} \partial_\mu \phi \partial_\nu \phi - V(\phi)\right]. \tag{1.34}$$

[6] The precise values depend on the specific details of reheating and the post-inflationary thermal history of the universe. The numbers we use here are a rough estimation.

The potential accounts for the self-interaction of the inflaton. Here we will not ask ourselves about the nature of the field ϕ; instead, we will use it as a clock that parametrizes the evolution of the energy density. Although in principle the inflaton could depend also on the position, $\phi(\boldsymbol{x}, t)$, the symmetries of the FLRW metric require that it must be homogeneous, i.e., $\phi(t)$.

Varying the action with respect to the metric we get the Friedmann equations for single field inflation

$$3M_P^2 H^2 = \frac{\dot{\phi}^2}{2} + V(\phi) \tag{1.35}$$

$$M_P^2 \dot{H} = -\frac{\dot{\phi}^2}{2}. \tag{1.36}$$

We can also infer what the density and the pressure are in terms of ϕ by identifying $T^0{}_0 = \rho$ and $T^i{}_j = -p\delta^i{}_j$ (cf. eq.(1.5)):

$$\rho = \frac{\dot{\phi}^2}{2} + V(\phi) \tag{1.37}$$

$$p = \frac{\dot{\phi}^2}{2} - V(\phi). \tag{1.38}$$

On the other hand, the variation of the action with respect to ϕ gives the Klein-Gordon equation

$$\ddot{\phi} + 3H\dot{\phi} + V_{,\phi} = 0, \tag{1.39}$$

where we the notation with the comma means, as usual,

$$V_{,\phi} \equiv \frac{\partial V}{\partial \phi}. \tag{1.40}$$

Now, let us prove that this model does indeed support inflation. In eqs.(1.22), (1.25) and (1.26) we wrote down three equivalent conditions an inflationary regime should fulfill. The one involving ϵ is the most useful one. In single field inflation it becomes

$$\epsilon = \frac{\dot{\phi}^2}{2M_P^2 H^2} < 1. \tag{1.41}$$

Therefore, making use of the Friedmann equation (1.35), we see that the condition for inflation is to have a potential energy that dominates over the kinetic one, that is:

$$\epsilon = \frac{3\dot{\phi}^2}{\dot{\phi}^2 + 2V} \simeq \frac{3\dot{\phi}^2}{2V}, \tag{1.42}$$

where the fact that $\epsilon < 1$ implies that the potential energy must dominate in the denominator; the approximation follows without further physical assumptions. Figure 1.8 shows an example of a potential that supports inflation.

So far, so good. But, as we recently showed, there is a further requirement: inflation should last long enough, i.e., about 60 efolds. It is obvious that if we want to keep $\epsilon < 1$ then it must not increase too quickly. In more precise terms, ϵ should not change much in one Hubble time, which means that the

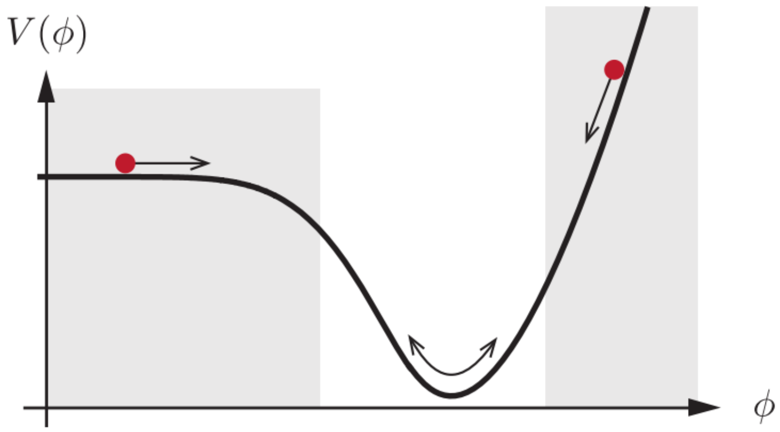

FIGURE 1.8: Example of a potential. Inflation may happen in the shaded region, where the kinetic energy of the field is much smaller than its potential energy. Picture taken from [2]

quantity $\frac{\dot\epsilon}{\epsilon H}$ must be small. We can push this condition a bit further to realize that

$$\frac{\dot\epsilon}{\epsilon H} = 2\left(\frac{\ddot\phi}{\dot\phi H} + \epsilon\right). \tag{1.43}$$

We see that if we wanted to sustain inflation for a long period of time then we would need both $\epsilon \ll 1$ and

$$\eta \equiv \frac{\ddot\phi}{\dot\phi H} \ll 1, \tag{1.44}$$

where we introduce a second parameter called η, in order to keep track of the rate at which ϵ changes.

Slow-roll approximation

So far no approximations have been made. We only pointed out that in a regime where both $\epsilon \ll 1$ and $\eta \ll 1$, inflation occurs and persists in time. In particular, there could be more models where these conditions were not realized, as inflation only needs $\epsilon < 1$. However, this regime of $(\epsilon, \eta) \ll 1$ looks very natural if we are to ask a prolonged epoch of inflation.

The *Slow-roll approximation* consists in using these conditions to simplify the equations of motion. $\epsilon \ll 1$ implies that $\frac{1}{2}\dot\phi^2 \ll V$, and $\eta \ll 1$ that $\ddot\phi \ll \dot\phi H$. These two result in the following approximated forms of the Friedmann equation (1.35) and the equation of motion for $\phi(t)$, eq.(1.39):

$$3M_P^2 H^2 \simeq V, \tag{1.45}$$

$$3H\dot\phi \simeq -V_{,\phi}\,. \tag{1.46}$$

Surprisingly enough, ϵ and η are called *slow-roll parameters*. The sentence "at first order in slow-roll", which will keep coming up in this work, means that terms proportional to second and higher powers of the slow-roll parameters have been neglected.

Although the slow-roll approximation is not the only possible mechanism for inflation (recall that the requirement for inflation is that $\epsilon < 1$; $(\epsilon, \eta) \ll 1$ is a further supposition), it is by far the most popular and well established one, perhaps because the resulting equations are very simple, but also because so far it is in agreement with the observations. In this work only these types of models will be considered.

Other models of inflation

When thinking about inflation, it has to be taken into account that it could have operated at a energy scale as high as 10^{15}GeV, far away from the physics reproducible in our accelerators[7]. That is why, despite the theoretical effort in, for instance, working out effective field theories of inflation, or trying to derive fundamental properties from string theory, the basic questions are still a mystery: what is the inflaton? Why did the universe start in such a high energy state? Our ignorance can be measured in the great number of available inflationary models that agree with observations. Although single field inflation is by far the simplest model, it is not the only way in which an inflationary epoch can be physically realized.

Let us, for instance, question the assumptions that were implicitly made in the single field action, eq. (1.34). Why should the field couple minimally to gravity? And why should we suppose that the field has a canonical kinetic term? Or, for that matter, why should we use Einstein gravity, given the extremely high energy scales involved? All these questions result in different models of single field inflation, none of which will play an important role in this thesis.

There is one group of models, though, around which this work will revolve considerably: multifield inflation. Of course, assuming the inflaton was the only dynamically relevant field during inflation was no more than a hypothesis, and there is no reason why we shouldn't, instead of eq.(1.34), consider an action that looks like

$$S = \int d^4x \sqrt{-g} \left[\frac{R}{2} + \frac{1}{2} g^{\mu\nu} \partial_\mu \phi^I \partial_\nu \phi_I - V(\phi^I) \right], \tag{1.47}$$

where the capital Latin index I labels the different possible fields.

There will be enough time to go deeper into multifield models of inflation later. For now, it is enough to bear in mind that several models of inflation are able to overcome the classical problems of the Big Bang model. In order to try to elucidate which one is the model that best suits our universe, we should make some more measurable predictions out of these theories. That is precisely the aim of the upcoming chapter.

[7] To be precise, the energy scale at which inflation happened is not constrained at all: It could range from 10^3GeV to 10^{15}GeV.

Chapter 2

Quantum fluctuations in inflation

We have presented inflation as a simple and elegant mechanism that allowed us to overcome the issue of the homogeneity and flatness of the universe without requiring a fine-tuned set of initial conditions. But what about the inhomogeneities? After all, the universe is not completely homogeneous –the fact that we, highly inhomogeneous carbon-based beings, exist is a undeniable proof. Perhaps the most exciting aspect of the inflationary theory is that, being introduced to explain homogeneity, is also able to explain the small inhomogeneities.

The general idea goes as follows. Quantum fluctuations $\delta\phi(\boldsymbol{x}, t)$ around the classical background of the inflaton field $\phi(t)$ make some regions of the universe end inflation slightly later or sooner than others. Thus, different parts undergo different evolutions; the quantum-level inhomogeneities are stretched by the great expansion of the universe and inhomogeneities become arbitrarily big. Hotter or colder spots in the CMB sky are the consequence of those quantum fluctuations in the early universe.

Before going into detail, a remark about the scope of the theory is in order here. As in any physical theory, one could start by expanding around the homogeneous universe up to first order. Linear treatment of the perturbations, nevertheless, ceases to be valid on small scales in the recent past. As S. Dodelson puts it, “we can never hope to understand cosmology by carefully examining rock formations on Earth”[9], but even the processes at intermediate scales –collapse of matter into a galaxy, star formation, etc.– are much too complicated to allow comparison between linear theory and observations. The best probe of small inhomogeneities with which our linear theories can make contact is again the CMB. And so our efforts will be directed towards trying to explain the small fluctuations in the Cosmic Microwave Background. How these fluctuations become galaxies and stars (eventually also rocks on Earth) is the concern of a different branch of Cosmology, and is out of the scope of the present work.

All these points will become much clearer in this chapter, which is largely based on [10], [11] and [12]. Although single field models of inflation are at the back of our minds for most of this chapter, many of the results are also valid in multifield scenarios. The latter will be discussed separately in section 2.4. But let us now begin from the beginning which is, as usual in physics, the harmonic oscillator.

2.1 Quantization of a massless scalar field in de Sitter

Although its title may suggest it, this is not merely an academic section. In section 2.3.3 it will be shown how cosmological perturbations can be related to the simpler problem of quantizing a massless scalar field in de Sitter. Thus, this section will provide most of the results needed to understand the relevant physics behind the origin of structure.

The action for the massless scalar field is given by

$$S = \int d^4x \sqrt{-g} \left(-\frac{1}{2} \partial_\mu \phi \partial^\mu \phi \right). \tag{2.1}$$

It will turn out to be more convenient to write the metric in terms of a conformal time τ instead of the cosmic time t, defined by

$$\tau = \int \frac{dt}{a(t)}, \tag{2.2}$$

where in the de Sitter case $a(t) = e^{-Ht}$, and thus

$$\tau = -\frac{1}{aH}. \tag{2.3}$$

The de Sitter metric with this conformal time is

$$ds^2 = a^2(\tau) \left(-d\tau^2 + d\boldsymbol{x}^2 \right), \tag{2.4}$$

The action for the massless scalar field in de Sitter spacetime is then

$$S = \frac{1}{2} \int d\tau d^3x \, a^2 \left(\phi'^2 - (\nabla \phi)^2 \right), \tag{2.5}$$

where a prime denotes a derivative with respect to the conformal time τ.

It is very similar to a harmonic oscillator. Thus, motivated by the fact that we know everything about harmonic oscillators in Minkowski spacetime, we try to get rid of the annoying scale factor a with the change of variables

$$u \equiv a\phi. \tag{2.6}$$

At first sight, it seems that have generated an unwanted term proportional to uu', but that can be fixed with an integration by parts, after which the action reads

$$S = \frac{1}{2} \int d\tau d^3x \left(u'^2 - (\nabla u)^2 + \frac{a''}{a} u^2 \right). \tag{2.7}$$

Now the first two term are the same as in Minkowski spacetime, and the fact that this scalar field is living in a de Sitter spacetime is represented by the third term, which can be seen as a time dependent effective mass $m_{\text{eff}}^2 = -a''/a$. The Fourier conjugate[1] of the field u is

$$u(\tau, \boldsymbol{x}) = \int \frac{d^3k}{(2\pi)^3} u_{\boldsymbol{k}}(\tau) e^{i\boldsymbol{k}\cdot\boldsymbol{x}}. \tag{2.8}$$

The function $u_k(\tau)$ has to satisfy the classical equation of motion in Fourier space. It turns out to be the equation for a harmonic oscillator with a time-dependent mass:

$$u_k'' + \left(k^2 - \frac{a''}{a} \right) u_k = 0. \tag{2.9}$$

By virtue of eq.(2.3) we have that

$$\frac{a''}{a} = \frac{2}{\tau^2}. \tag{2.10}$$

[1]See section 2.3.1 to look at our choice of normalization of the Fourier conjugates.

Thus, the mode equation is

$$u_k'' + \left(k^2 - \frac{2}{\tau^2}\right) u_k = 0. \tag{2.11}$$

Let us continue by employing the standard quantization techniques upon the field u. First, we promote it to a quantum field $\hat{u}$ and we expand it in Fourier space,

$$\hat{u}(\tau, \boldsymbol{x}) = \int \frac{d^3k}{(2\pi)^3} \{u_k(\tau)\hat{a}_{\boldsymbol{k}} e^{i\boldsymbol{k}\cdot\boldsymbol{x}} + u_k^*(\tau)\hat{a}_{\boldsymbol{k}}^\dagger e^{-i\boldsymbol{k}\cdot\boldsymbol{x}}\}. \tag{2.12}$$

Alternatively, the Fourier components u_k are promoted to operators and expressed as

$$u_{\boldsymbol{k}} \to \hat{u}_{\boldsymbol{k}} = u_k(\tau)\hat{a}_{\boldsymbol{k}} + u_{-k}^*(\tau)\hat{a}_{-\boldsymbol{k}}^\dagger, \tag{2.13}$$

where $\hat{a}^\dagger$ and $\hat{a}$ are the usual creation and annihilation operators, satisfying the canonical commutation relations

$$[\hat{a}_{\boldsymbol{k}}, \hat{a}_{\boldsymbol{k'}}] = \left[\hat{a}_{\boldsymbol{k}}^\dagger, \hat{a}_{\boldsymbol{k'}}^\dagger\right] = 0 \qquad \text{and} \qquad \left[\hat{a}_{\boldsymbol{k}}, \hat{a}_{\boldsymbol{k'}}^\dagger\right] = (2\pi)^3\delta(\boldsymbol{k} - \boldsymbol{k'}). \tag{2.14}$$

These commutation relations are satisfied if and only if the mode functions u_k are normalized as follows:

$$\langle u_k, u_k \rangle \equiv \frac{i}{\hbar}(u_k^* u_k' - u_k^{*\prime} u_k) = 1. \tag{2.15}$$

Our aim is to solve the equation (2.11). As is the case for any second order differential equation, we need two boundary conditions. The first is given by eq.(2.15), but we still need another one. Let us look for more information in the vacuum states.

The vacuum state $|0\rangle$ is the state annihilated by $\hat{a}_{\boldsymbol{k}}$, i.e.,

$$\hat{a}_{\boldsymbol{k}}|0\rangle = 0. \tag{2.16}$$

As we just said, the mode functions $u_k(\tau)$ are not completely specified by the solution of their equation of motion. Thus, there is no unique notion of the vacuum; different choices for $u(\tau)$ give different vacuum solutions. Or, in other words, the choice of vacuum is our second boundary condition.

What vacuum should we choose? Well, to make a proper choice we should have more information about the physics involved in the problem. This will become clear later, when we discuss the cosmological perturbations. So the question remains open for the time being.

There is one last thing we can compute now that will become handy later on. The mean square expectation value of the operator $\hat{u}_{\boldsymbol{k}}$ in the ground state, i.e., the zero-point function, is

$$\langle|\hat{u}_{\boldsymbol{k}}^2|\rangle = \langle 0|\hat{u}_{\boldsymbol{k}}^\dagger \hat{u}_{\boldsymbol{k}}|0\rangle \tag{2.17}$$

$$= \langle 0| \left(u_k(\tau)\hat{a}_{\boldsymbol{k}} + u_{-k}^*(\tau)\hat{a}_{-\boldsymbol{k}}^\dagger\right) \left(u_{-k}^*(\tau)\hat{a}_{-\boldsymbol{k}}^\dagger + u_k(\tau)\hat{a}_{\boldsymbol{k}}\right) \hat{u}_{\boldsymbol{k}}|0\rangle \tag{2.18}$$

$$= |u_k(\tau)|^2, \tag{2.19}$$

where in the second line we have used eq.(2.13), and in the third line we played with the commutation relations of the creation-annihilation operators.

Enough warming-up. It is time to tackle the real physical problem, that is, how to describe cosmological perturbations. The driver warns you: it is quite a long trip. Are you ready?

2.2 Cosmological perturbation theory

In order to study cosmological perturbations we can split all quantities $X(t, \boldsymbol{x})$ into the background value $\bar{X}(t)$ and small perturbations $\delta X(t, \boldsymbol{x})$, that is,

$$X(t, \boldsymbol{x}) = \bar{X}(t) + \delta X(t, \boldsymbol{x}). \tag{2.20}$$

What kind of quantities should we perturb? Well, there are some that come quickly to our mind. The energy density ρ, whose perturbations $\delta\rho$ are observed in the CMB is perhaps the most obvious one. We also have the pressure p or the inflaton ϕ. Anything else? Sure thing. Einstein Equations tell us that matter (or rather the energy-momentum tensor $T_{\mu\nu}$) is coupled to gravity. Therefore, a consistent approach must take into account both perturbations to the energy-momentum tensor and to the metric. This is getting complicated.

Let us try to simplify the problem. At the time of recombination the universe was even more homogeneous and flatter than what it is now, so supposing background homogeneity and flatness is all the more justified. Moreover, given that the observed perturbations in the CMB are so small, expanding the Einstein Equations at linear order,

$$\delta G_{\mu\nu} = 8\pi G \; \delta T_{\mu\nu}. \tag{2.21}$$

will certainly approximate the full solution to very high accuracy.

So now we have a strategy: write the linearized version of the Einstein Equations and try to solve them. Following the notation used in Chapter 5 of S. Weinberg's *Cosmology* book [10], the most general perturbed metric can be written as[2]

$$ds^2 = -(1+E)dt^2 + aJ_i dx^i dt + a^2 \left[(1-2\psi)\delta_{ij} + H_{ij}\right] dx^i dx^j, \tag{2.22}$$

where some properties of the new functions introduced will be detailed below. The full metric is a sum of the homogeneous FLRW metric and a linear perturbation $h_{\mu\nu}$, i.e.,

$$g_{\mu\nu} = \bar{g}_{\mu\nu} + h_{\mu\nu}. \tag{2.23}$$

On the other hand, perturbations to the energy-momentum tensor after inflation are

$$\delta T_{ij} = \bar{p}\, h_{ij} + a^2 \delta_{ij} \delta p, \quad \delta T_{i0} = \bar{p}\, h_{i0} - (\bar{\rho} + \bar{p})\delta u_i, \quad \delta T_{00} = -\bar{\rho}\, h_{00} + \delta\rho \tag{2.24}$$

With these complicated forms it is not yet easy to see why solving the linearized Einstein Equations is the good strategy to follow. It is the aim of the following sections to show how calculations can be sweetened up.

[2] As most of the computations involved are algebraically quite heavy, I encourage the interested reader to check S. Weinberg's text whenever this one becomes too vague.

2.2.1 SVT decomposition

We have an ace up the sleeve: the FLRW background is highly symmetric. If we decompose all the quantities we have introduced into scalar (S), vectors (V) and tensors (T), then homogeneity and isotropy of the background ensure that the perturbations of each type evolve independently, i.e., they are not coupled in the equations of motion.[3]

The SVT decomposition for the vectors and tensors in the metric is the following:

$$J_i = \partial_i F - G_i, \qquad \text{with } \partial^i G_i = 0 \tag{2.25}$$

$$H_{ij} = \partial_{ij} B + \partial_i C_j + \partial_j C_i + D_{ij}, \tag{2.26}$$

where

$$\partial^i C_i = 0, \quad D_{ij} = D_{ji}, \quad D^i_i = 0, \quad \partial^i D_{ij} = 0. \tag{2.27}$$

The decomposition of the vector, sometimes called Helmholtz decomposition, splits the 3 degrees of freedom of the spatial vector into a divergence-free vector, G_i, and a rotational-free part, $\partial_i F$. The tensor H_{ij} has been decomposed into a symmetric, traceless and transverse tensor D_{ij}, a divergence-free vector C_j and a scalar B. We can do a quick check to verify that the ten degrees of freedom of the original metric $\delta g_{\mu\nu}$ are still there. After the decomposition we have four scalars, two divergence-free vectors and one symmetric, traceless and transverse tensor. In total, $(4 \times 1) + (2 \times (3-1)) + (1 \times (6-1-3)) = 10$ degrees of freedom.

The decomposition for the vectorial and tensorial quantities appearing in the perturbation to the energy-momentum tensor is completely analogous. Following Weinberg [10], we get

$$\delta T_{00} = -\bar{\rho} h_{00} + \delta\rho \tag{2.28}$$

$$\delta T_{i0} = \bar{p} h_{i0} - (\bar{\rho} + \bar{p})\left(\partial_i \delta u + \delta u_i^V\right) \tag{2.29}$$

$$\delta T_{ij} = \bar{p} h_{ij} + a^2 \left[\delta_{ij}\delta p + \partial_i \partial_j \pi^S + \partial_i \pi_j^V + \partial_j \pi_i^V + \pi_{ij}^T\right]. \tag{2.30}$$

As mentioned, once the perturbations have been decomposed this way, the Einstein Equations decouple in the three modes and it is easier to study them. Vector perturbations such as G_i, C_i or δu_i^V are not created by inflation, and even if they were, they decay with the expansion of the universe. Hence, we will ignore them in this work. Tensor fluctuations are the cause of primordial gravitational waves we are still eager to observe, for instance, via polarization of the CMB. In fact, there is only one Einstein Equation for the tensor modes and it is the wave equation for gravitational radiation,

$$-16\pi G a^2 \pi_{ij}^T = \nabla^2 D_{ij} - a^2 \ddot{D}_{ij} - 3a\dot{a}\dot{D}_{ij}. \tag{2.31}$$

The scalar modes, on the other hand, are the most complicated, involving eight scalars and several Einstein Equations relating them. One can check Weinberg [10] to see that the equations for the scalar perturbations, even after the SVT decomposition, are still fearsomely complicated. But we are very interested in solving them: the will to explain density fluctuations in the CMB, which are scalar fluctuations of the density, is what brought us here. The following sections are all about trying to get an equation of motion for the scalar perturbation, something analogous to eq. (2.31).

[3] There are some ways to proof this statement, each one with a higher degree of sophistication. Baumann gives a proof in the appendix of [11], and Weinberg[10] just writes all the equations of motion and checks there is no coupling between the different modes.

2.2.2 Gauge freedom

There are more degrees of freedom in the background plus perturbations equations than there are physical degrees of freedom. We would like to identify which of those are truly physical.

This problem did not exist before, when we only considered the homogeneous universe, because the symmetries of the FLRW made the coordinate choice so distinguished that we never worried about it. Actually, in any other system of coordinates than the one we chose the universe would not look homogeneous nor isotropic. But now that the perturbations introduce inhomogeneities, there is no preferred reference frame. Furthermore, if we are not careful with the choice of coordinates, we can produce unphysical or fictitious perturbations. To make this point sharper, let us consider a universe where the energy density is only a function of time in some coordinates, $\rho(t,\boldsymbol{x}) \doteq \rho(t)$, that is, it is homogeneous and isotropic. Let us introduce some new spatial coordinates $\tilde{\boldsymbol{x}} = \boldsymbol{x} + \delta\boldsymbol{x}(t,\boldsymbol{x})$. The homogeneous and isotropic universe is not so in the new reference frame, since $\tilde{\rho}(t,\tilde{\boldsymbol{x}}) = \rho(t,\boldsymbol{x}(t,\boldsymbol{x}))$. These perturbations are not physical, but only due to the inappropriate choice of coordinates.

Coordinate transformations can also be seen, from a different perspective, as *gauge transformations* of the fields. For instance, under a infinitesimal coordinate transformation (we here drop the spacetime indices for clarity)

$$x \to x' = x + \epsilon(x), \tag{2.32}$$

where $\epsilon(x)$ is small in the same sense that the perturbations are small[4], a scalar field $\rho(x)$ changes as

$$\rho(x) \to \rho'(x') = \rho(x(x')) = \rho(x' - \epsilon(x')). \tag{2.33}$$

At linear order in perturbations the Taylor expansion gives, after dropping the primes,

$$\rho(x) \to \rho'(x) = \rho(x) - \epsilon(x)\partial_x\phi(x), \tag{2.34}$$

so the coordinate transformations can be seen as a transformation of the field while leaving the coordinates untouched. It is more useful to think about coordinate transformations as gauge transformations in disguise, as the latter only affect the perturbations, while the former affect both the perturbations and the background.

Let us use the gauge freedom to simplify our task as much as we can. There are several gauge choices one can make. I will mention some of them here, which will be of particular interest for later reference.

- **Uniform density gauge** As its name suggests, it is defined by

$$\delta\rho = 0 \qquad \text{and} \qquad B = 0. \tag{2.35}$$

- **Comoving gauge** This is the gauge in which the scalar momentum density vanishes

$$\delta u = 0 \qquad \text{and} \qquad B = 0. \tag{2.36}$$

  In this gauge the inflaton is spatially uniform, that is,

$$\delta\phi(t,\boldsymbol{x}) = \delta\phi(t), \tag{2.37}$$

[4] This ϵ does not have anything to do with the slow-roll parameter introduced in the previous chapter. Well, it does: both have to be small.

and all the spatial perturbations are described by the metric.

- **Flat gauge** The gauge where the spatial part of the metric is flat, i.e.,

$$\psi = 0 \qquad \text{and} \qquad B = 0. \tag{2.38}$$

Fixing the gauge is not the only possibility: there is another –complementary– strategy we can follow in order to avoid the pitfall of fictitious gauge modes. We can work with gauge invariant quantities which, by definition, are equivalent in any gauge. The two crucial gauge invariant quantities to describe cosmological perturbations created by inflation are ζ and $\mathcal{R}$.

2.2.3 The curvature perturbations ζ and $\mathcal{R}$

Definitions and choices

As we shall learn later in this chapter, the curvature perturbation ψ becomes very important when describing the origin of structure from quantum fluctuations during inflation. It seems reasonable that in different gauges this quantity will take different values, and it is customary to give them special names. They are usually denoted by ζ and $\mathcal{R}$.

A quick skim through the literature shows that there is no consensus in the question of what gauge should each one correspond to. Up to now, for the reasons mentioned in the introduction to section 2.2, we have worked up to linear order in perturbations. Those reasons are still valid now, and will be throughout the remaining of this thesis. Nevertheless, for some calculations related with non-gaussianities of the power spectrum –these terms may sound strange to the unexperienced reader, but they will be properly presented in section 2.3.1– it is necessary to have ζ and $\mathcal{R}$ defined at least up to second order. While the focus of this work will be on calculations where the linear order is enough, it is still interesting to explore the possible conventions at all orders and adopt the one that we think is the most natural.

We will employ the notation

$$g = g_0 + g_1 + \frac{1}{2} g_2 \tag{2.39}$$

to split a generic quantity g into its background value and first and second order perturbations.

Here comes our definition: we shall denote by ζ_1 the curvature perturbation at linear order in *uniform density* gauge, and by $\mathcal{R}_1$ when in the *comoving* gauge. More explicitly:

$$-\zeta_1 = \psi_1^{\text{uniform-density gauge}} \tag{2.40}$$

$$\mathcal{R}_1 = \psi_1^{\text{comoving gauge}}. \tag{2.41}$$

Up to this point, and up to the minus sign, the majority of authors agree (see, however, [13]). The divergence in the definitions comes at second and higher order in perturbation theory. The one we find more robust and enticing is the one introduced by Salopek and Bond [14] and thereafter used by many more authors, which consists on identifying ζ and $\mathcal{R}$ with ψ (give or take a minus sign) also at higher orders in perturbation theory.

For such an identification to make sense, we need a perturbed metric that is also valid at higher order in perturbation theory. We can write the spatial part of the metric in the form

$$\gamma_{ij} = a^2(t) e^{-2\psi} \delta_{ij}, \tag{2.42}$$

where at first order

$$e^{-2\psi} = 1 - 2\psi + \mathcal{O}(\psi^2) \tag{2.43}$$

and we recover the spatial part of the metric as given at linear order in eq.(2.22).

Thus, our definitions *at all orders* are simply

$$\zeta \equiv -\psi^{\text{uniform-density gauge}} \tag{2.44}$$

$$\mathcal{R} \equiv \psi^{\text{comoving gauge}}, \tag{2.45}$$

together with the right form of the metric (2.42). To be completely explicit, the spatial part of the metric in the uniform-density gauge would read

$$\gamma_{ij} = a^2(t)(1 + 2\zeta)\delta_{ij} \tag{2.46}$$

at first order in perturbations, and

$$\gamma_{ij} = a^2(t)(1 + 2\zeta + 2\zeta^2)\delta_{ij} \tag{2.47}$$

at second order. Analogous expressions follow for the comoving gauge by interchanging ζ by $-\mathcal{R}$.

As was mentioned above, this thesis will only use the first order results. Nevertheless, the discrepancy in notations found in the literature makes a clear-cut definition almost necessary. As an example of different notation, some other authors (see for instance [15]) choose to use (2.46) as a definition of ζ even at higher orders.

Gauge invariant expressions

Once ζ and $\mathcal{R}$ have been properly defined, we can give their gauge invariant expressions.

The gauge-invariant quantity for ζ at first order is

$$\zeta_1 = -\psi_1 - H\frac{\delta\rho_1}{\dot{\rho}_0}, \tag{2.48}$$

and that for $\mathcal{R}_1$ is

$$\mathcal{R}_1 = \psi_1 - H\frac{\delta\phi}{\dot{\phi}}, \tag{2.49}$$

where the subscripts have the meaning given in eq. (2.39).

This statement can be proven by noting that, under an infinitesimal coordinate transformation

$$x^\mu \to x'^\mu = x^\mu + \epsilon^\mu(x) \tag{2.50}$$

the quantities involved transform as follows[16],[10]:

$$\psi_1 \to \psi_1 - H\epsilon_0 \tag{2.51}$$
$$\delta\rho_1 \to \delta\rho_1 + \dot{\rho}_0\epsilon_0. \tag{2.52}$$

Thus, under a general coordinate transformation

$$\zeta = -\psi_1 - H\frac{\delta\rho_1}{\dot{\rho}_0} \to -\psi_1 + H\epsilon_0 - \frac{H}{\dot{\rho}_0}\left(\delta\rho_1 + \dot{\rho}_0\epsilon_0\right) = \tag{2.53}$$
$$= -\psi_1 - H\frac{\delta\rho_1}{\dot{\rho}_0} \tag{2.54}$$

is invariant. Similar computations follow for $\mathcal{R}$.

If one is a thrill-seeker and is smart enough to add and subtract the right quantities, it is possible to find the second order gauge invariant quantity, as they did in [17]:

$$\zeta_2 = -\psi_2 - \mathcal{H}\frac{\delta\rho_2}{\rho_0'} + 2\mathcal{H}\frac{\delta\rho_1}{\rho_0'}\frac{\delta\rho_1'}{\rho_0'} + 2\frac{\delta\rho_1}{\rho_0'}\psi_1' - \left(\mathcal{H}\frac{\delta\rho_1}{\rho_0'}\right)^2\left(\frac{\rho_0''}{\mathcal{H}\rho_0'} - \frac{\mathcal{H}'}{\mathcal{H}^2} - 2\right). \tag{2.55}$$

Note that this expression still obeys our definition (2.44), since $\zeta_2 = -\psi_2$ in the uniform-density ($\delta\rho = 0$) gauge.

Conservation outside of the horizon

In section 1.3 we introduced the concept of the Hubble radius or Hubble horizon. We will use the terms *inside* and *outside* the horizon[5] to describe length scales which are causally connected or disconnected at given time, i.e., smaller or bigger than the Hubble horizon $(aH)^{-1}$. It is much more common to think about this concepts in terms of the Fourier conjugates of the length, the wavenumbers k:

$$\text{subhorizon: } k > aH \qquad\qquad \text{superhorizon: } k < aH. \tag{2.56}$$

We *defined* inflation as an epoch of shrinking Hubble radius. The idea is that virtually all perturbations that begin inside exit the horizon at some given time. Those modes remain unaffected by causal physics until the Hubble radius grows enough and they re-enter.

Here comes the crux of the matter. As we will show in a second, ζ and $\mathcal{R}$ are conserved outside of the horizon. In particular, they are not affected by the unknown physics of Reheating. Hence, if we could measure any quantity that is related to ζ or $\mathcal{R}$ nowadays, we would be able to trace the information all the way back into the quantum fluctuations during inflation. And, in fact, there is something related to the spatial scalar perturbations that we can measure: the CMB anisotropies.

Let us go with the proof. The first who realized that $\mathcal{R}$ and ζ were conserved in superhorizon scales was S. Weinberg[6]. It is worth taking a look at his proof either in his book [10] or in [16]. We will, however, follow a simpler reasoning mentioned, for instance, in [18]. They show that at first

[5] In this section, and almost throughout the whole thesis, we will use the word "horizon" as a synonym for Hubble horizon. Do not confuse it with the particle horizon; the whole point of inflation was to make them different!

[6] Actually, the conservation of these specific quantities on superhorizon scales was discovered by Salopek and Bond in the 1980s. Weinberg formulated a theorem that generalized their result.

order in perturbations and in *gradient expansion*,[7] and with the adiabaticity condition $p = p(\rho)$, the conservation equation reads

$$\dot{\rho} + 3\left(H + \dot{\psi}_1|_{B=0}\right)(\rho + p) = 0, \tag{2.57}$$

where the gauge condition $B = 0$ has been specified. (Note that the gauge is not completely fixed yet, and that the expression is valid at all three gauges (2.35), (2.36) and (2.38).) At zeroth order in perturbations it is just the continuity equation, eq. (1.6). Therefore, the equation at first order in perturbations is

$$\dot{\psi}_1|_{B=0} = 0 \qquad \text{outside of the horizon.} \tag{2.58}$$

In the uniform-density and comoving gauges, using the definitions (2.40) and (2.41) we get the important result that, provided the adiabatic condition $p = p(\rho)$ is satisfied, ζ_1 and $\mathcal{R}_1$ are conserved outside the horizon.

2.3 Contact with observations

2.3.1 Statistics

The normalization of the Fourier transform we use is the following:

$$f_{\boldsymbol{k}} = \int d^3x\, e^{-i\boldsymbol{k}\cdot\boldsymbol{x}} f(\boldsymbol{x}), \tag{2.59}$$

$$f(\boldsymbol{x}) = \int \frac{d^3k}{(2\pi)^3}\, e^{i\boldsymbol{k}\cdot\boldsymbol{x}} f_{\boldsymbol{k}}. \tag{2.60}$$

This implies that the Dirac delta function is

$$\delta_D(\boldsymbol{k}) = \int \frac{d^3x}{(2\pi)^3} e^{\pm i\boldsymbol{k}\cdot\boldsymbol{x}}. \tag{2.61}$$

We will make use of two-point correlation functions of a quantity $\mathcal{R}(\boldsymbol{x})$,

$$\xi_{\mathcal{R}}(\boldsymbol{r}) \equiv \langle \mathcal{R}(\boldsymbol{x})\mathcal{R}(\boldsymbol{x} + \boldsymbol{r})\rangle. \tag{2.62}$$

Note that by homogeneity ξ depends only on the distance, not the direction of $\boldsymbol{r}$, i.e.,

$$\xi_{\mathcal{R}}(\boldsymbol{r}) = \xi_{\mathcal{R}}(r) \tag{2.63}$$

We now consider the correlation function $\langle \mathcal{R}_{\boldsymbol{k}}\mathcal{R}_{\boldsymbol{k}'}\rangle$, related to the real space one by a Fourier transformation[8]

[7] The gradient expansion method is a prescription to expand superhorizon quantities perturbatively in an orderly fashion. The expansion is performed in powers of the ratio $\epsilon \equiv \frac{k}{aH}$, which is considered to be small. Thus, by "first order in gradient expansion" what is meant is "linear approximation on superhorizon scales".

[8] It is worthwhile mentioning that it is spatial homogeneity what makes the Fourier transformation of a correlation function to be proportional to a delta function, that is,

$$\langle \mathcal{R}(x_1)\cdots\mathcal{R}(x_n)\rangle = \langle \mathcal{R}(x_1 + z)\cdots\mathcal{R}(x_n + z)\rangle \implies \langle \mathcal{R}_{k_1}\cdots\mathcal{R}_{k_n}\rangle \propto \delta_D\left(k_1 + \cdots + k_n\right). \tag{2.64}$$

$$\langle \mathcal{R}_{\boldsymbol{k}} \mathcal{R}_{\boldsymbol{k}'} \rangle = \int d^3x e^{-i(\boldsymbol{k}+\boldsymbol{k}')\cdot \boldsymbol{x}} \int d^3r \xi_{\mathcal{R}}(r) e^{-i\boldsymbol{k}\cdot\boldsymbol{r}} \tag{2.65}$$

$$= (2\pi)^3 \delta_D(\boldsymbol{k}+\boldsymbol{k}') \int d^3r \xi_{\mathcal{R}}(r) e^{-i\boldsymbol{k}\cdot\boldsymbol{r}}. \tag{2.66}$$

The power spectrum of a quantity $\mathcal{R}$ is *defined* as the Fourier transform of the two point correlation function

$$P_{\mathcal{R}}(k) \equiv \int d^3r \xi_{\mathcal{R}}(r) e^{-i\boldsymbol{k}\cdot\boldsymbol{r}}. \tag{2.67}$$

And so, we get

$$\langle \mathcal{R}_{\boldsymbol{k}} \mathcal{R}_{\boldsymbol{k}'} \rangle = (2\pi)^3 \delta_D(\boldsymbol{k}+\boldsymbol{k}') P_{\mathcal{R}}(k). \tag{2.68}$$

It is also usual to work with the quantity

$$\Delta^2_{\mathcal{R}}(k) \equiv \frac{k^3}{(2\pi)^2} P_{\mathcal{R}}(k). \tag{2.69}$$

For Gaussian perturbations all high order correlation functions can be expressed in terms of the two-point function, and therefore all the information is contained in the power spectrum. The lowest order non-Gaussian features can be measured by the three point function

$$\langle \mathcal{R}_{\boldsymbol{k}_1} \mathcal{R}_{\boldsymbol{k}_2} \mathcal{R}_{\boldsymbol{k}_3} \rangle = (2\pi)^3 B_{\mathcal{R}}(k_1, k_2, k_3) \delta_D(\boldsymbol{k}_1 + \boldsymbol{k}_2 + \boldsymbol{k}_3), \tag{2.70}$$

known as the *Bispectrum*. Non-Gaussian features of the CMB lie outside the scope of the present work.

2.3.2 Measurable quantities and numerical values

The measurable quantities have to do with the correlation functions introduced in the previous section. We now list the most useful parameters that we can get from experiment, and their numerical values as measured by the Planck Collaboration [19].

- **Scalar power spectrum** Δ^2_s. Planck value:

$$\ln(10^{10}\Delta^2_s) = 3.089 \pm 0.036 \text{ (68\%CL)}, \tag{2.71}$$

  this is,

$$\Delta^2_s \simeq 2.2 \times 10^{-9}. \tag{2.72}$$

- **Scalar spectral tilt** $n_s - 1$.

  It is defined by

$$n_s - 1 \equiv \frac{d \ln \Delta^2_s}{d \ln k}, \tag{2.73}$$

  where the minus one appears there for historical reasons. Note that if the spectrum was scale invariant then $n_s = 1$.

  Planck value:

$$n_s - 1 = -0.0345 \pm 0.0062 \text{ (68\%CL)}, \tag{2.74}$$

which corresponds to an almost scale invariant power spectrum.

This is the most conclusive measurement in favor of slow-roll models. Further down in this chapter we see (take a look at eq. (2.106)) that slow-roll models predict a small deviation from scale invariance, agreeing with this observational result. It is also the most powerful reason to why the second slow-roll parameter η is constrained to be so small.

- **Tensor to scalar ratio,** r. It is defined by

$$r \equiv \frac{\Delta_t^2}{\Delta_s^2}. \tag{2.75}$$

Constraints coming from Planck, BICEP and Keck array together give the upper bound of

$$r < 0.07 \text{ (95\%CL)}. \tag{2.76}$$

- **Tensor spectral tilt**. Similarly, it is given by

$$n_t \equiv \frac{d \ln \Delta_t^2}{d \ln k}, \tag{2.77}$$

this time without the minus one sign. Of course, primordial gravitational waves have not been observed yet, but other measurements constrain it to be

$$n_t < 0.014(95 \tag{2.78}$$

- **Running of the tilt**. Planck value

$$\frac{dn_s}{d \ln k} = -0.0057 \pm 0.0071 \text{ (68\%CL)} \tag{2.79}$$

2.3.3 Theoretical results in single field slow-roll

The moment to gather all the information laid down in the previous –quite boring, I'm afraid– sections and to build something useful out of it has arrived.

Let us begin by counting the scalar degrees of freedom there are. We have four in the perturbed metric (E, F, ψ and B), and four more on the matter side. But they are related via six Einstein Equations, so that only two of them remain unspecified. Then, as we are working on single field inflation, we have $\delta\phi$ (if we were considering multifield inflation with N scalar fields, then we would have all the N scalar degrees of freedom $\delta\phi_1 \cdots \delta\phi_N$). By fixing the gauge in any of the ways shown in section 2.2.2 we kill two more scalar degrees of freedom. Hence, the counting goes as presented in Table 2.1.

	Metric	Inflaton	Gauge choice	Constraints	**True d.o.f**
Scalars	4	1	-2	-2	**1**
Tensors	2	0	0	0	**2**

TABLE 2.1: Counting scalar and tensor degrees of freedom.

After all this work we have learnt that scalar cosmological perturbations are described by a single degree of freedom, and that tensorial perturbations by two. The interpretation of the tensorial d.o.f. is clear: they correspond to the two polarizations modes of the primordial gravitational waves. The objective now is to characterize the scalar degree of freedom, find its equation of motion and, if possible, relate it to the observed phenomena. We have a couple of really good candidates to do the job: ζ and $\mathcal{R}$. Any of the two could be used , since we only have to calculate their values when they crossed the horizon, for they remain unaltered until horizon re-entry. The references we follow, [11] and [10] choose to use $\mathcal{R}$, and we will stick to that choice.

Weinberg, in chapter 10 of his book [10] does all the work for us. It is a bit too heavy on the algebraic side, and thus we prefer to leave it to the interested reader. He finds the following equation governing the sub horizon evolution of $\mathcal{R}$

$$\mathcal{R}_k'' + 2\frac{z'}{z}\mathcal{R}_k' + k^2\mathcal{R}_k = 0, \tag{2.80}$$

sometimes called the *Mukhanov-Sasaki* equation.

Introducing the *Mukhanov* variable

$$v \equiv z\mathcal{R}, \qquad \text{where } z^2 \equiv a^2\frac{\dot{\phi}^2}{H^2} \tag{2.81}$$

and Fourier-expanding it with the normalization given in section 2.3.1, we arrive at

$$v_k'' + \left(k^2 - \frac{z''}{z}\right)v_k = 0. \tag{2.82}$$

This equation should ring a bell. It has the same form as the equation for the massless field in de Sitter, eq. (2.11)!

Power spectrum of scalar perturbations

So far, we have been hopping between references [10] and [11]. But now we have to make a choice, as their methods for the computation of the power spectrum diverge. The two possible paths are the following:

Since equation (2.82) is impossible to solve for a general $z(\tau)$, Baumann [11] takes the purely de Sitter limit, where

$$\frac{z''}{z} = \frac{a''}{a} = \frac{2}{\tau^2}. \tag{2.83}$$

We thus have

$$v_k'' + \left(k^2 - \frac{2}{\tau^2}\right)v_k = 0, \tag{2.84}$$

which is exactly equation (2.11).

However, the reader might be concerned about the fact that inflation is not necessarily described by a purely de Sitter spacetime ($\epsilon = 0$), as was shown in 1.3.2, but rather by $\epsilon \ll 1$. Baumann argues that taking the purely de Sitter limit is justified if the quantities appearing in the power spectrum are evaluated at horizon crossing, but it is not trivial to see why this should be the case. On the other hand, Weinberg writes and solves equation (2.80) at linear order in slow-roll parameters, i.e.,

$$\mathcal{R}_k'' - \frac{2(1+\eta+\epsilon)}{\tau}\mathcal{R}_k' + k^2\mathcal{R}_k = 0. \tag{2.85}$$

We will stick to the easier-to-follow de Sitter limit Baumann takes. (For the full computation using eq.(2.85) and its solution in terms of Hankel functions, the reader is encouraged to check chapter 10 of [10]). Of course, the resulting power spectrum is the same no matter which way it is calculated.

One of the reasons of going for the de Sitter approximation is that in section 2.1 we already did most of the work. We stopped because we needed physical information to choose a vacuum, but we can get that information now. Note that the wavelength associated with a given mode k can always be found inside the Hubble radius provided one goes sufficiently backwards in time, since the comoving Hubble radius was shrinking during inflation. For a wavelength smaller than the Hubble radius the influence of the curvature can be neglected and the mode evolves as if it was in Minkowski spacetime. In other words, for $\tau \to -\infty$ or $k \gg aH$, eq.(2.82) gives

$$v_k'' + k^2 v_k = 0, \tag{2.86}$$

which is nothing but the equation of a simple harmonic oscillator. Finally, an equation we know how to solve! From the two solutions we choose the one with the positive frequency. Our second boundary condition will be

$$\lim_{\tau \to -\infty} v_k = \frac{e^{-ik\tau}}{\sqrt{2k}}, \tag{2.87}$$

which in the jargon of quantum field theory on curved spacetimes is called *Bunch-Davies vacuum.*

Let us look back to the equation we want to solve, eq.(2.82). It can be checked that

$$v_k = \alpha \frac{e^{-ik\tau}}{\sqrt{2k}} \left(1 - \frac{i}{k\tau}\right) + \beta \frac{e^{ik\tau}}{\sqrt{2k}} \left(1 + \frac{i}{k\tau}\right) \tag{2.88}$$

is a solution to the equations. The two boundary conditions, eqs.(2.15) and (2.87), impose that $\alpha = 1$ and $\beta = 0$, so that the unique mode functions are

$$v_k = \frac{e^{-ik\tau}}{\sqrt{2k}} \left(1 - \frac{i}{k\tau}\right). \tag{2.89}$$

We now have all the ingredients to calculate the power spectrum of $\mathcal{R}_k$. First note that

$$\langle \mathcal{R}_k \mathcal{R}_{k'} \rangle = \frac{H^2}{\dot{\phi}^2} \frac{\langle v_k v_{k'} \rangle}{a^2}, \tag{2.90}$$

because only the modes v_k depend on k. So we only need to calculate $\langle v_k v_{k'} \rangle$ to get the two-point correlation function of $\mathcal{R}_k$. Using our brand new solution, eq.(2.89), we get

$$\frac{\langle v_k v_{k'} \rangle}{a^2} = (2\pi)^3 \delta_D(\boldsymbol{k} + \boldsymbol{k}') \frac{H^2}{2k^3} (1 + k^2\tau^2). \tag{2.91}$$

On superhorizon scales , $k \gg aH$ or $|k\tau| \ll 1$ this approaches a constant

$$\frac{\langle v_k v_{k'} \rangle}{a^2} \to (2\pi)^3 \delta_D(\boldsymbol{k} + \boldsymbol{k}') \frac{H^2}{2k^3}. \tag{2.92}$$

$$\langle \mathcal{R}_k \mathcal{R}_{k'} \rangle = (2\pi)^3 \delta_D(\boldsymbol{k} + \boldsymbol{k}') \frac{H_*^4}{2k^3 \dot{\phi}_*^2}, \tag{2.93}$$

where the subscript $*$ denotes that quantities should be evaluated at horizon crossing $a(t_*)H(t_*) = k$.

Together with eq.(1.41) and definitions (2.68) and (2.69) we get

$$\Delta_s^2 \equiv \Delta_{\mathcal{R}}^2 = \frac{1}{8\pi^2} \frac{H_*^2}{M_P^2} \frac{1}{\epsilon_*}, \tag{2.94}$$

where we have used the label s to denote scalar perturbations and we reintroduced the Planck mass for later convenience.

Power spectrum of tensor perturbations

The hard work is already done; the calculation of the power spectrum of the tensor modes will appear almost trivial. For scalar field theories the anisotropic inertia π_{ij}^T appearing in equation (2.31) vanishes. Then, in Fourier space we have

$$\ddot{D}_k + 3H\dot{D}_k + \frac{k^2}{a^2} D_k = 0. \tag{2.95}$$

In terms of the conformal time defined in eq.(2.2) we get the by now familiar equation

$$D_k'' + 2\frac{a'}{a} D_k' + k^2 D_k = 0. \tag{2.96}$$

Yes, it is the Mukhanov-Sasaki equation (2.80), except that z is replaced with a. Performing the change of variables $v_k \equiv aD_k$ we once again get eq. (2.9). The computation of the power spectrum proceeds in complete analogy to the scalar sector with one small caveat: there are two polarization modes, and therefore we should add up their contributions. The power spectrum of the tensor fluctuations created by inflation is

$$\Delta_t^2 = 2 \times \frac{1}{\pi^2} \frac{H_*^2}{M_P}. \tag{2.97}$$

Other quantities

We now compute some of the quantities mentioned in section 2.3.2 in the slow-roll approximation.

The most straightforward to compute is the tensor to scalar ratio, defined in eq.(2.75). It is given by

$$r = 16\epsilon_*, \tag{2.98}$$

where the star denotes, once again, that the quantity is to be evaluated at horizon crossing.

We can also compute the spectral tilts at first order in slow-roll. The scalar spectral tilt, defined in eq.(2.74) can be calculated via

$$n_s - 1 = \frac{d \ln \Delta_s^2}{dN} \frac{dN}{d \ln k}, \tag{2.99}$$

where N is the number of efolds, defined in (1.32). The first term is easy to compute. Using the result of eq.(2.94) it follows that

$$\frac{d \ln \Delta_s^2}{dN} = 2\frac{d \ln H}{dN} - \frac{d \ln \epsilon}{dN}. \tag{2.100}$$

Now, the first term is just -2ϵ, as is clear by using the definition of N and ϵ:

$$2\frac{d \ln H}{dN} = 2\frac{d \ln H}{dt} \frac{dt}{dN} = 2\frac{\dot{H}}{H^2} = -2\epsilon. \tag{2.101}$$

For the second one we need to recall the definition of the second slow-roll parameter η, given in eq.(1.44):

$$\frac{d\ln\epsilon}{dN} = \frac{\dot{\epsilon}}{\epsilon H} = 2\epsilon + 2\eta. \tag{2.102}$$

So that the first term of eq.(2.99) is

$$\frac{d\ln\Delta_s^2}{dN} = -4\epsilon - 2\eta. \tag{2.103}$$

The second term of that same equation is computed by recalling that we are evaluating the quantity at horizon crossing, i.e., $k = aH$. Hence, we have

$$\ln k = N + \ln H, \tag{2.104}$$

and

$$\frac{dN}{d\ln k} = \left(\frac{d\ln k}{dN}\right)^{-1} = (1-\epsilon)^{-1} = 1 + \epsilon + \mathcal{O}(\epsilon^2). \tag{2.105}$$

Thus, at first order in slow-roll we find

$$n_s - 1 = -4\epsilon_* - 2\eta_*. \tag{2.106}$$

Analogous computations lead to a similar result for the tensor spectral tilt:

$$n_t = -2\epsilon_*. \tag{2.107}$$

It is interesting to note that the single field slow-roll models satisfy the consistency relation

$$r = -8n_t, \tag{2.108}$$

which will be of some relevance below.

2.4 Multifield. δN formalism

When calculating the power spectrum from quantum fluctuations during inflation, there is a crucial difference between single field and multifield models. In section 2.2.3 we stressed that the curvature perturbations ζ and $\mathcal{R}$ are conserved outside of the horizon only if the so-called adiabaticity condition $p = p(\rho)$ is satisfied. It turns out that this condition is not satisfied when the universe is filled with more than one scalar field. And so, we need to find a procedure to take into account their evolution when they leave the horizon, that lead to *non-adiabatic* perturbations that leave potentially measurable traces on the power spectrum.

In this section we present the δN formalism, which will turn out to be a powerful technique to calculate not only the Gaussian quantities in multifield inflation, but also deviations from gaussianity such as the bispectrum. We do so by following [20], [18] and [21].

Our starting point will be the ADM (Arnowitt-Deser-Misner) metric[22], another standard way to decompose the metric

$$ds^2 = -\alpha^2 dt^2 + \gamma_{ij}(dx^i + \beta^i dt)(dx^j + \beta^j dt), \tag{2.109}$$

where γ_{ij} can be decomposed as

$$\gamma_{ij} = a^2 e^{-2\psi}(e^h)_{ij} \tag{2.110}$$

without loss of generality. The scale factor a and its scalar perturbation ψ are the same quantities introduced above. The traceless tensor h_{ij} can be further decomposed as

$$h_{ij} = \partial_i C_j + \partial_j C_i - \frac{2}{3}\delta_{ij}\partial_k C^k + h_{ij}^{(T)}, \tag{2.111}$$

where C_i contains both scalar and vector perturbations and $h_{ij}^{(T)}$ is the part containing tensor perturbations.

In this setting the flat and uniform-density gauges defined in section 2.2.2 become

$$\text{flat gauge: } \psi = C_i = 0, \tag{2.112}$$

and

$$\text{uniform-density gauge: } \delta\rho = C_i = 0. \tag{2.113}$$

The generic definition of ζ given in eq. (2.44) still holds, i.e., it is the value, up to a minus sign, of the curvature perturbation ψ in the uniform-density gauge. In the ADM metric this means

$$\zeta \equiv -\psi|_{\delta\rho = C_i = 0}. \tag{2.114}$$

It is time to prove the core idea of the δN formalism: ζ and the number of efolds are related by a gauge transformation from the flat gauge to the uniform-density gauge.

Under a change of coordinates given by $t \to \hat{t}$ and $x^i \to \hat{x}^i$, the number of efolds defined in eq.(1.32) changes simply as

$$N = \ln\left(\frac{a(t)}{a(t_i)}\right) \to \hat{N} = \ln\left(\frac{a(\hat{t}\,)}{a(t_*)}\right), \tag{2.115}$$

where t_i is an arbitrary initial time and the hat denotes that the quantity is evaluated in the uniform-density gauge. We call δN to the difference between the number of e-folds computed in the flat gauge and that computed in the uniform-density gauge, this is,

$$\delta N \equiv N - \hat{N}, \tag{2.116}$$

On the other hand, in [18] they show that the spatial part of the metric transforms, on large scales, in the following way

$$\gamma_{ij}|_{C_i=0}(t, \boldsymbol{x}) = \hat{\gamma}_{ij}|_{C_i=0}(\hat{t}, \hat{\boldsymbol{x}}), \tag{2.117}$$

where the condition $C_i = 0$, common to both gauges, has already been applied.

Remembering the decomposition of eq.(2.110) and taking determinant and logarithm in both sides of eq. (2.117) we find that

$$\psi_{ij}|_{C_i=0}(t, \boldsymbol{x}) = \hat{\psi}_{ij}|_{C_i=0}(\hat{t}, \hat{\boldsymbol{x}}) + \ln\left(\frac{a(t)}{a(\hat{t}\,)}\right). \tag{2.118}$$

Specializing this result for a gauge transformation from the flat gauge to the uniform density gauge

$$\hat{\psi}_{ij}|_{\delta\rho=C_i=0}(\hat{t},\hat{\boldsymbol{x}}) = \ln\left(\frac{a(\hat{t}\,)}{a(t)}\right). \tag{2.119}$$

Equations (2.115) and (2.119) are remarkably similar. They imply that the relation between ζ and δN is very simple:

$$\zeta \equiv -\hat{\psi}_{ij}|_{\delta\rho=C_i=0}(\hat{t},\hat{\boldsymbol{x}}) = \ln\left(\frac{a(t)}{a(t_i)}\right) - \ln\left(\frac{a(\hat{t}\,)}{a(t_i)}\right) = N - \hat{N} \equiv \delta N. \tag{2.120}$$

Let us connect this result with the scalar perturbations created during inflation. One can take t_* as the time, during inflation, at which some scale k exited the Hubble radius, that is, $k_* = a(t_*)H(t_*)$, and t_e as the time when inflation ends[9]. With this in mind, eq.(2.116) becomes

$$\delta N(t_*, t_e, \boldsymbol{x}) = N(t_*, t_e) - \hat{N}(t_*, t_e, \boldsymbol{x}). \tag{2.121}$$

Now, $\hat{N}$ can be seen as a function of the fields $\phi^I(t_*, \boldsymbol{x})$ on the flat hypersurface. In principle, and this is an important comment in the present work, it could also depend on the velocities of the fields, $\dot{\phi}^I(t_*, \boldsymbol{x})$, but it is assumed that during inflation every field obeys an equation of motion in the slow-roll approximation, that is,

$$3H\dot{\phi}^I \simeq -\frac{\partial V(\phi^I)}{\partial \phi_I} \tag{2.122}$$

Indeed, if this is the case, we can trade $\dot{\phi}^I$ for ϕ^I by using eq.(2.122), and therefore $N(\phi^I, \dot{\phi}^I) = N(\phi^I)$. One of the conclusions of this thesis questions the validity of this assumption in the broader multifield slow-roll scenario that will be introduced below. But, for the time being, let us accept it and see where it takes us to.

Moreover, one can split the fields into a homogeneous background and a perturbation

$$\phi^I(t_*, \boldsymbol{x}) = \phi^I(t_*) + \delta\phi^I(t_*, \boldsymbol{x}). \tag{2.123}$$

Then, it is a matter of expanding δN in series of the initial field perturbations $\delta\phi^I(t_*, \boldsymbol{x})$:

$$\zeta = \delta N(t_c, t_*, \boldsymbol{x}) = \sum_I \frac{\partial N}{\partial \phi^I_*}\delta\phi^I_* + \frac{1}{2}\sum_{I,J}\frac{\partial^2 N}{\partial\phi^I_*\partial\phi^J_*}\delta\phi^I_*\delta\phi^J_* + \mathcal{O}(\delta\phi^3). \tag{2.124}$$

This is the δN formalism, which allows us to relate ζ to the initial perturbations of the scalar fields, provided that we know the derivatives of the number of efolds with respect to the fields.

Now we can compute the power spectrum. Taking each $\delta\phi^I$ to be uncorrelated with one another at early times, we get

$$\langle \delta\phi^I_{\boldsymbol{k}}\delta\phi^J_{\boldsymbol{k'}}\rangle = (2\pi)^3\,\delta^{IJ}\,\delta_D(\boldsymbol{k}+\boldsymbol{k'})\mathcal{P}_*(k), \qquad \text{where } \mathcal{P}_*(k) = \frac{H_*^2}{2M_P k^3} \tag{2.125}$$

and where the Kronecker delta appears because they are uncorrelated.

[9]By setting t_e to be the time after inflation ends we are assuming that the quantities that we observe are not affected by whatever happens after inflation. In particular, they are blind to the specific process of reheating. Further information available in [21].

The power spectrum for ζ is defined analogously,

$$\langle \zeta_{\boldsymbol{k}} \zeta_{\boldsymbol{k'}} \rangle = (2\pi)^3 \, \delta_D(\boldsymbol{k}+\boldsymbol{k'}) \mathcal{P}_\zeta(k). \tag{2.126}$$

Using eq.(2.124) we get that

$$\langle \zeta_{\boldsymbol{k}} \zeta_{\boldsymbol{k'}} \rangle = \sum_{I,J} N_I N_J \langle \delta\phi^I_{\boldsymbol{k}} \delta\phi^J_{\boldsymbol{k'}} \rangle, \tag{2.127}$$

where a comma stands for a partial derivative, that is,

$$N_{,I} \equiv \frac{\partial N}{\partial \phi^I}. \tag{2.128}$$

This gives the following result for the power spectrum of the scalar fluctuations:

$$\Delta^2_\zeta \equiv \Delta^2_s = \sum_I N^2_{,I} \Delta^2_* = \sum_I N^2_{,I} \frac{H^2_*}{4\pi^2}. \tag{2.129}$$

Another interesting quantity is the scalar spectral tilt, which was defined in eq.(2.73). Following the same steps as in section 2.3.3 we get, to first order in slow-roll,

$$n_s - 1 \equiv \frac{d\ln \mathcal{P}_s}{d\ln k} = \frac{d\ln \mathcal{P}_\zeta}{d\ln k} \simeq \frac{1}{H}\frac{d\ln \mathcal{P}_\zeta}{dt}. \tag{2.130}$$

Using eq.(2.129) and interchanging each time derivative for a derivative with respect to the fields, this is,

$$\frac{d}{dt} = \sum_J \dot{\phi}^J \frac{\partial}{\partial \phi^J}, \tag{2.131}$$

one obtains

$$n_s - 1 = -2\epsilon + \frac{2}{H} \frac{\sum_{I,J} \dot{\phi}^J N_{,IJ} N_{,I}}{\sum_K N^2_{,K}}. \tag{2.132}$$

One of the main appeals of the δN formalism is its power to compute non-Gaussianities in a simple manner. For instance, the bispectrum, defined in (2.70) gives

$$B(k_1,k_2,k_3) = 4\pi^2 \mathcal{P}^2_\zeta \frac{\sum_i k_i^3}{\prod_i k_i^3} \left(\frac{-\mathcal{F}(k_1,k_2,k_3)}{4M_P^2 \sum_K N^2_{,K} \sum_i k_i^3} + \frac{\sum_{I,J} N_{,I} N_{,J} N_{,IJ}}{\left(\sum_K N^2_{,K}\right)^2} \right), \tag{2.133}$$

where $\mathcal{F}$ has the following form

$$\mathcal{F}(k_1,k_2,k_3) = -\sum_{i\neq j} k_i k_j^2 - \frac{8}{k_1+k_2+k_3} \sum_{i>j} k_i^2 k_j^2 + \sum_i k_i^3. \tag{2.134}$$

As was mentioned, this is not a big part of the present work, and we only show the result. Further details may be found in [21].

2.5 Summary and discussion

Quite a lot of work has been done in this chapter. But, at the end of the day, the relevant quantities can be counted on the fingers of one hand. For single field slow-roll models, we got the scalar and tensorial power spectra, given in equations (2.94) and (2.97), as well as their spectral tilts, in eqs. (2.106) and (2.107). On the multifield side we computed, once again, the power spectrum for scalar fluctuations and its tilt, as can be read out in equations (2.129) and (2.132), by means of the δN formalism[10].

These are the most important results because, as we learnt in section 2.3.2, they are the ones that can be compared with observations. And what do observations say? Can we answer the primordial question of whether it was a single field or multiple fields that drove inflation? The answer is no... yet. Presently, the measurements are not conclusive in favoring single or multifield. However, the hope is that in the near future improved measurements will allow us to make much more precise statements about the origin of the universe. In particular, there are some measurements that would falsify single field inflation: large non-gaussianity, this is, a sizeable contribution from the bispectrum, non-zero *isocurvature* perturbations[11], and/or violating the single field consistency relation given in equation (2.108).

Let us focus in the last one, for both r and n_t are already constrained by experiment, as can be checked in section 2.3.2. For convenience, let us rephrase here what we said earlier in the text. By comparing eqs.(2.98) and (2.107), the following consistency relation for single field slow-roll models arises:

$$r = -8n_t. \tag{2.135}$$

Can we derive a similar constraint for multifield inflation? The answer is affirmative, and can have far-reaching consequences. The necessary computations are carried out in Appendix A, and the resulting multifield consistency relation is given by equation (A.5):

$$r = -8n_t \cos^2 \alpha, \tag{2.136}$$

where α is the angle between the gradient of the number of efolds and the velocity of the fields.

This result is thought-provoking. First of all, does it make sense to introduce such an angle? Well, as we are dealing with multifield models that evolve along the gradient of the potential (cf. eq. (2.122)), the number of efolds until the end of inflation $N(\phi)$ can be computed for any value of ϕ. Furthermore, multifield inflation can be *defined* to be precisely the set of models in which $\alpha \neq 0$. This might be striking at first glance, as one tends to think about multifield inflation as the models in which more than one scalar fields are present in the action. But what if all scalar fields are extremely light and do not change at all the way inflation happens? Those models, although based on multiple fields, behave effectively as single field models. The definition we propose here does precisely that: it distinguishes between *effective* models of single and multiple fields by introducing the angle α.[12]

[10]The power spectrum for tensorial fluctuations and its tilt are the same in multifield and single field models of inflation. The reason for this is that scalar and tensorial modes decouple with the SVT decomposition, and thus, adding more scalar fields does not affect the equations of motion for the tensorial fluctuations, eq.(2.96).

[11]These perturbations, also called *non-adiabatic*, are the ones that happen in the perpendicular directions to which the field is moving. Of course, such fluctuations are only possible in multifield models of inflation (in single field there is only one direction in field space). Although it was not mentioned in the text explicitly, they can be computed by employing the δN formalism.

[12]This suggestive idea is not followed in the rest of the text, and multifield inflation is defined in the usual "more than one scalar field in the action" way.

The second immediate conclusion is that this is a relation that could be experimentally tested in the upcoming future. New measurements could be able to tell if the relation (2.135) holds or if, on the contrary, it is suppressed by the cosine factor in eq.(2.136).

The last reason why equation (2.136) is exciting is that it is new. As far as we know, it has never been mentioned in the literature before.

Chapter 3

Multifield slow-roll under suspicion

In this chapter we first review some multifield slow-roll paradigms appeared in the literature. Following I.-S. Yang's work [23], we discuss why none of them is completely satisfactory. This criticism results in a better understanding of the slow-roll trajectories in multifield models of inflation, and our own interpretation of the right parameters –which differs from that given by I.-S. Yang– is presented at the end of the chapter.

3.1 Reviewing the slow-roll conditions

This section starts by delving further into the single slow-roll inflation that was presented in 1.3.3, introducing the *potential* slow-roll parameters. Afterwards, a generalization to multifield models based on [23] is performed. It will be argued why such a generalization is not trivial, and some choices appeared in the literature will be analyzed.

3.1.1 Single field inflation

What we learnt there was that our focus is on models of inflation where the first two slow-roll conditions

$$\epsilon \equiv -\frac{\dot{H}}{H^2} = \frac{\dot{\phi}^2}{2H^2} \simeq \frac{3}{2}\frac{\dot{\phi}^2}{V} \ll 1 \qquad \text{and} \qquad \eta \equiv \frac{\ddot{\phi}}{\dot{\phi}H} \ll 1, \tag{3.1}$$

also known as *Hubble slow-roll* conditions, are satisfied. Note that the approximation in ϵ follows directly by using the Friedmann equation (1.35) and by the requirement that $\epsilon \ll 1$; no other assumptions are involved.

In section 1.3.3 we learnt that within the slow-roll approximation the equation of motion of the fields becomes

$$\dot{\phi} \simeq -\frac{V'}{3H}. \tag{3.2}$$

One of the consequences of the slow-roll approximations is that the slow-roll parameters can be written only in terms of the potential. When they are written in such a way they are called *potential* slow-roll parameters.

The first potential slow-roll parameter can be computed using (3.1) and (3.2):

$$\epsilon = \frac{\dot{\phi}^2}{2M_P^2 H^2} \simeq \frac{M_P^2 V'^2}{2V^2} \equiv \epsilon_V. \tag{3.3}$$

On the other hand, requiring the approximation 3.2 to be consistent with the field equation of motion, eq.(1.39), implies that

$$\ddot{\phi} = -\partial_t \left(\frac{V'}{3H} \right) \ll V', \tag{3.4}$$

which leads us to

$$\frac{1}{3} \left(\frac{V''}{V} - \epsilon \right) \ll 1. \tag{3.5}$$

Thus, it is natural to define

$$\eta_V \equiv M_P^2 \frac{V''}{V} \ll 1 \tag{3.6}$$

as the potential second slow-roll parameter.

The fact that the slow-roll parameters can be expressed in terms of the potential is one of the main reasons why slow-roll models are so popular: given any potential it is straightforward to determine whether or not the slow-roll parameters are small at a given point, and hence whether or not inflation is supported. Thus, it makes the study of specific models of inflation almost trivial when the derivative of the potential are known.

A small warning note is in order here. The Hubble and potential slow-roll parameters are not equivalent. While $\epsilon < 1$ is the definition of inflation, $\epsilon_V < 1$ is a necessary but not sufficient condition. To make this statement more clear, consider a case in which $\epsilon_V < 1$, yet the kinetic energy of the field is larger than the potential. In such a case, inflation does not happen because, no matter what ϵ_V is, ϵ is greater than 1. A similar reasoning leads one to conclude that a small η_V does not necessarily make ϵ stay small during inflation. The statement, then, is that Hubble and potential slow-roll parameters contain the same information whithin the slow-roll approximation, this is, when the approximated equation of motion (3.2) accurately describes the behavior of the field.

3.1.2 A generalization to multifield inflation

A generalization of the slow-roll parameters will be carried out in this section following I.-S. Yang's cited work. As will become clear in section 3.2.2, from our point of view this is not a correct way of understanding the multifield slow-roll paradigm. However, it is very instructive to see this approach first.

The multifield models that we are going to treat in this section have a canonical kinetic term and minimal coupling. These models of inflation arise from an action that was already written down in 1.3.3: eq. (1.47). This time each field ϕ^I evolves according to the single field equation of motion (1.39), i.e.,

$$\ddot{\phi}^I + 3H\dot{\phi}^I + \delta^{IJ} V_{,J} = 0, \tag{3.7}$$

where the fact that the kinetic term is canonical (as opposed to some models we will consider later) is represented by the delta function and the partial derivatives. The Friedmann equations are now,

$$3M_P^2H^2 = \frac{\dot{\phi}^I\dot{\phi}^J\delta_{IJ}}{2} + V(\phi^I), \tag{3.8}$$

$$M_P^2\dot{H} = -\frac{\dot{\phi}^I\dot{\phi}^J\delta_{IJ}}{2}, \tag{3.9}$$

which are very similar to the single field equations (1.35) and (1.36).

The first slow-roll condition in its Hubble version is a trivial generalization of the single field case:

$$\epsilon \equiv -\frac{\dot{H}}{H^2} = \frac{(\dot{\phi}^I)^2}{2M_P^2H^2}. \tag{3.10}$$

Although $\dot{\phi}^I$ is a vector now, we only care about its magnitude. Something similar must happen with the potential version of the parameter,

$$\epsilon \simeq \frac{M_P^2}{2}\frac{(V_{,I})^2}{V^2} \equiv \epsilon_V. \tag{3.11}$$

Once more, we only care about the magnitude of $V_{,I}$.[1]

However, when considering the same generalization for the second slow-roll parameter, a problem arises. While for ϵ and ϵ_V it was clear that the norms of the vectors $\dot{\phi}^I$ and $V_{,I}$ must be taken, it is not clear how should η and η_V in eqs.(3.1) and (3.6) be generalized to the multifield case.

Well, η still has the phenomenological meaning we gave to it on section 1.3.3, namely that of ensuring that ϵ stays small long enough. In other words, η is a parameter that makes

$$\frac{\dot{\epsilon}}{\epsilon H} \ll 1. \tag{3.12}$$

Thus, one can compute an equation analogous to the single field relation (1.43):

$$\frac{\dot{\epsilon}}{\epsilon H} = 2\epsilon + \frac{\ddot{H}}{\dot{H}H} = 2\left(\epsilon + \frac{\ddot{\phi}^I\dot{\phi}^J\delta_{IJ}}{\left(\dot{\phi}^K\right)^2 H}\right), \tag{3.13}$$

and so it is natural to identify η with the quantity

$$\eta \equiv \frac{\ddot{\phi}^I\dot{\phi}^J\delta_{IJ}}{\left(\dot{\phi}^K\right)^2 H}. \tag{3.14}$$

Note that this relation reduces to that of eq.(3.1) for a single field.

The real trouble comes with η_V. Equation (3.6) cannot be generalized right away to the multifield case, since what in single field was V'' is now a matrix, $\partial_I\partial_J V$. It is not clear what part of that matrix should be taken to be small.

One of the main points of this thesis is to work out what the proper slow-roll parameters are. By learning to interpret them we might as well learn something new about the dynamics of multifield inflation. For now, let us follow I.-S. Yang's criticism of a couple of conditions appeared in the literature.

[1] Beware! This expression is in contradiction with what we think is the true first potential slow-roll parameter, which will be introduced in **??**

3.1.3 Bad choices appeared in the literature

Sasaki and Stewart, in their ground-breaking work [20], suppose that the trace of the matrix $\partial_i \partial_j V$ needs to be small, i.e.,

$$\frac{M_P^2 \sqrt{(\partial_I \partial_J V)(\partial_J \partial_I V)}}{V} \ll 1. \tag{3.15}$$

This condition is sufficient but not necessary, as I.-S. Yang shows with the following example.

Take a two field potential of the form

$$V(\phi, \psi) = V(\phi) + \frac{m^2}{2}\psi^2, \tag{3.16}$$

where $V(\phi)$ is a potential that supports the usual single field slow-roll inflation. In such a case, a large mass term m^2 at points where $\psi = 0$ ruins the condition (3.15) right away. And yet, we know that ordinary single field inflation will happen via the potential $V(\phi)$.

Another popular –yet still incorrect– condition is the one that states that each component of the acceleration in eq. (3.7) should be negligible , this is,

$$|\ddot{\phi}^I| \ll |3H\dot{\phi}^I| \text{ or } |V_{,I}|, \qquad \text{for every component } I. \tag{3.17}$$

Understanding why this condition is wrong is a crucial issue in this thesis. Without specifying a specific coordinate system, each component of the vector is physically meaningless. To make this point sharper, let us consider two reference frames (ϕ, ψ) (ϕ', ψ') rotated with respect to each other. Let us choose the gradient of the potential, ∇V, to be along the ϕ axis. Say that the condition (3.17) works when we describe the problem in the primed fields. Nevertheless, it cannot work in the (ψ, ϕ) frame. Here is why: as the gradient of the potential goes along the ϕ axis, $|V_{,\psi}| = 0$, and there is no way in which $|\ddot{\psi}| \ll |V_{,\psi}|$. We conclude that condition (3.17) is a condition that depends on the choice of the coordinate frame, and therefore not applicable in general.

It was this idea that triggered our investigation process. Could we describe multifield inflation in a framework that was invariant under general field redefinitions? If that was the case, perhaps we would be able to say something about the slow-roll conditions that could apply to any reference frame.

3.2 Covariant multifield formalism

In this section, based on the work [24], we will present a framework that allows to write the expressions involved in multifield modes of inflation in a *covariant* way. Eventually, we will also present our thoughts and computations for the slow-roll conditions in multifield inflation.

3.2.1 A large class of multifield models

Let us try to write the most general multifield action that we can think of. The only constraints that we put are (i) that we are going to rely on Einstein gravity –even if it is not a true theory in the highest energy scale, we can still think of it as a very precise low-energy effective theory–, and (ii) that we will only consider scalar fields. With that information, the most generic multifield action we can write is

$$S = \int d^4x\sqrt{-g}\left(\frac{R}{2} + P(X,\phi^I)\right), \tag{3.18}$$

where P is an arbitrary function of the N scalar fields $\phi^1 \cdots \phi^N$ and of the kinetic term

$$X \equiv -\frac{1}{2}G_{IJ}\, g^{\mu\nu}\nabla_\mu\phi^I\nabla_\nu\phi^J. \tag{3.19}$$

There are already some interesting features that can be discussed at this point. One of them is that this action allows for non-trivial kinetic terms. Indeed, it is a generalized version of *k-inflation* or the *DBI inflation*. The potential is also encoded in the function $P(X,\phi^I)$, and there are no *a priori* restrictions on it. But the most enticing feature for our purposes is the field-space metric G^{IJ}. The logic works pretty much in the same way as it does with spacetime coordinates in General Relativity: redefinitions of the fields also transform the metric in a certain way, so that all expressions we may write down are invariant under general transformations of the fields.

A quick note on the notation employed: $g^{\mu\nu}$ is the spacetime metric (which we will assume to be of the FLRW form soon enough) and the usual Greek indices are used for spacetime coordinates, whilst the lower case Latin characters $i,j,k,\dots = 1,2,3$ are the spatial indices. On the other hand, G^{IJ} is the mentioned metric in the field space and the capital Latin letters $I,J,K,\dots = 1,\cdots,N$ are field indices. Moreover, ∇_μ stands for the covariant derivative in spacetime sector.

With some effort, one can compute the equations of motion that the action (3.18) produces. From the variation of the action with respect to ϕ^I one finds

$$\nabla_\mu(P_{,X}G_{IJ}\nabla^\mu\phi^J) - \frac{1}{2}(\nabla_\mu\phi^K)(\nabla^\mu\phi^L)\partial_I G_{KL} + P_{,I} = 0, \tag{3.20}$$

where $P_{,X}$ and $P_{,I}$ are the partial derivatives of P with respect to X and ϕ^I, respectively.

The energy-momentum tensor is of the form

$$T^{\mu\nu} = Pg^{\mu\nu} + P_{,X}G_{IJ}\nabla^\mu\phi^I\nabla^\nu\phi^J. \tag{3.21}$$

In FLRW spacetime the energy-momentum tensor reduces to the perfect fluid form of eq.(1.5) with an energy density

$$\rho = 2XP_{,X} - P \tag{3.22}$$

and pressure P –hence the name of the function.

Scalar fields must have an homogeneous background, so that $\phi^I(t,\boldsymbol{x}) = \phi^I(t)$ and

$$X = \frac{1}{2}G_{IJ}\dot\phi^I\dot\phi^J. \tag{3.23}$$

The Friedmann equations are also slightly altered

$$H^2 = \frac{2XP_{,X} - P}{3M_P^2} \tag{3.24}$$

$$M_P^2\dot H = -XP_{,X}. \tag{3.25}$$

And the equations of motion for the fields, given in eq.(3.20) become

$$\ddot{\phi}^I + \Gamma^I_{JK}\dot{\phi}^J\dot{\phi}^K + \left(3H + \frac{\dot{P}_{,X}}{P_{,X}}\right)\dot{\phi}^I - \frac{G^{IJ}P_{,J}}{P_{,X}} = 0, \tag{3.26}$$

where Γ^I_{JK} are the Christoffel symbols associated to the field-space metric G^{IJ}, and their definition is analogous to the customary in General Relativity:

$$\Gamma^I_{KL} \equiv \frac{1}{2}G^{IJ}(\partial_K G_{IL} + \partial_L G_{IK} - \partial_I G_{KL}). \tag{3.27}$$

Motivated by the fact that the first two terms of eq.(3.26) are very similar to the components of the acceleration in curved coordinates, it is appealing to define a new derivative, analogous to the *directional covariant derivative* of General Relativity:

$$D_t V^I \equiv \frac{DV^I}{dt} \equiv \partial_t V^I + \Gamma^I_{JK}V^J\dot{\phi}^K, \tag{3.28}$$

where V^I is a general vector. Another way of looking at it is

$$D_t V^I = \frac{d\phi^J}{dt}\nabla_J V^I, \tag{3.29}$$

where ∇_J is the usual covariant derivative, but acting on the field space. In other words, this is the covariant derivative *along the curve* $\phi^J(t)$, the background field trajectory, where t is the parameter that parametrizes the curve.

The resemblance with General Relativity is not superficial, and one can use all the machinery available. For instance, the vector V^I is parallel transported along the path $\phi^J(t)$ when its directional covariant derivative along that curve vanishes, i.e.,

$$D_t V^I = 0 \qquad \text{or} \qquad \partial_t V^I + \Gamma^I_{JK}V^J\dot{\phi}^K = 0. \tag{3.30}$$

This derivative has a couple convenient features. First of all, it is metric-compatible with respect to the field space metric, i.e.,

$$D_t G^{IJ} = 0. \tag{3.31}$$

Second of all, it acts as an ordinary time derivative on field space scalars (this is, quantities without field space indices):

$$D_t X = \partial_t X. \tag{3.32}$$

Making use of this derivative equation (3.26) becomes

$$D_t\dot{\phi}^I + \left(3H + \frac{\dot{P}_{,X}}{P_{,X}}\right)\dot{\phi}^I - \frac{G^{IJ}P_{,J}}{P_{,X}} = 0, \tag{3.33}$$

or in an even more compact form,

$$a^{-3}D_t(a^3P_{,X}\dot{\phi}_I) = P_{,I}. \tag{3.34}$$

Thus, it is natural to interpret eq. (3.33) as the geodesic equation for a particle in field space in the presence of two external forces: a frictional force proportional to the velocity of the fields, $\left(3H + \frac{\dot{P}_{,X}}{P_{,X}}\right)\dot{\phi}^I$, and a conservative force $\frac{G^{IJ}P_{,J}}{P_{,X}}$.

Slow-roll parameters

Once this general framework has been set up, we can ask ourselves what the true multifield slow-roll conditions are like. From equations (3.8) and (3.9) we can compute the first Hubble slow-roll parameter

$$\epsilon \equiv -\frac{\dot{H}}{H^2} = \frac{3XP_{,X}}{2XP_{,X} - P}. \tag{3.35}$$

And the second follows from

$$\frac{\dot{\epsilon}}{\epsilon H} = 2\epsilon + \frac{\partial_t(XP_{,X})}{HXP_{,X}}, \tag{3.36}$$

where we can identify η as

$$\eta \equiv \frac{\partial_t(XP_{,X})}{HXP_{,X}}. \tag{3.37}$$

The meaning behind these equations is somewhat obscured by the presence of the arbitrary function $P(X, \phi^I)$. Since non-trivial kinetic terms do not seem to add anything essential to our discussion about the slow-roll parameters, we had better simplify all these equations to the case with a trivial kinetic term: $P(X, \phi^I) = X + V$. Then again, sticking to the covariant notation will prove to be helpful.

3.2.2 $P(X, \phi^I) = X + V$

In this simple and habitual case, the action of eq.(3.18) simplifies to

$$S = \int d^4x\sqrt{-g}\left(\frac{R}{2} + \frac{1}{2}G_{IJ}\dot{\phi}^I\dot{\phi}^J - V(\phi^I)\right), \tag{3.38}$$

which can be understood as a generalization of the single field action (1.34) to the multifield case.

With $P(X, \phi^I) = X + V$ we also get that $P_{,X} = 1$, and so the new forms of the main equations presented in the previous section are, in units where

$$3H^2 = 2X - P, \tag{3.39}$$

$$\dot{H} = -X, \tag{3.40}$$

for the Friedmann equations, and

$$D_t\dot{\phi}^I + 3H\dot{\phi}^I + G^{IJ}V_{,J} = 0, \tag{3.41}$$

for the field equations of motion.

The key insight will be obtained by taking the dot product of $\dot{\phi}^I$ times each one of the equations of motion (3.41). This gives

$$\dot{X} + 6HX + V_{,K}\dot{\phi}^K = 0, \tag{3.42}$$

which is the same equation as the energy conservation equation (1.6) with $\rho = X - V$ and $P = X + V$.

Slow-roll conditions

The slow-roll parameters of equations (3.35) and (3.37) particularize to

$$\epsilon = \frac{3X}{X+V} \simeq \frac{3X}{V}, \tag{3.43}$$

$$\eta = \frac{\dot{X}}{XH}, \tag{3.44}$$

where the approximation in eq.(3.43) follows only from knowing that ϵ must be small. As was the case in single field, no further assumptions are involved.

Equation (3.44) tells us that the proper multifield slow-roll approximation is to drop the first term in the equation of motion (3.42), i.e.,

$$\dot{X} \ll 6HX \simeq -V_{,K}\dot{\phi}^K. \tag{3.45}$$

In particular, it should be noted that this is not the same as dropping the first term of equation (3.41), since

$$\dot{X} = G_{IJ}\dot{\phi}^I D_t\dot{\phi}^J, \tag{3.46}$$

and so there are two ways to make this quantity small. One is the typical slow-roll approach, where $D_t\dot{\phi}^I$ is small in norm; the other one is that, without being small, its projection onto $\dot{\phi}^I$ is small. This equation is, in our opinion, the correct multifield slow-roll approximation.

Potential slow-roll parameters

We can try to compute the slow-roll parameters in terms of the potential, as we did in single field. The upshot of this treatment is the same as in single field models: we would be able to tell, just by looking at the potential, if inflation will or won't happen.

In the previous section we learnt that the equation of motion that gives meaningful answers to these kind of questions is eq. (3.42), which in the slow-roll approximation is (3.45). In close analogy to the single field case, we can always solve the field equation of motion to find $\dot{\phi}^I$ in terms of V in the slow-roll regime:

$$|\dot{\phi}|^2 \simeq -V + \sqrt{V^2 + \frac{2}{3}|V'|^2\cos^2\varphi}, \tag{3.47}$$

where the other solution for $|\dot{\phi}|$ is negative and thus unphysical. The angle φ that we just introduced is the angle between $\dot{\phi}^I$ and the gradient of the potential, i.e.,

$$\cos\varphi \equiv \frac{\dot{\phi}^I V_{,I}}{|\dot{\phi}||V'|}. \tag{3.48}$$

Now we can compute the first potential slow-roll parameter. Combining eq.(3.43) and the solution (3.47)

$$\epsilon \simeq \frac{3X}{V} \simeq \frac{3}{2V}\left(-V + \sqrt{V^2 + \frac{2}{3}|V'|^2\cos^2\varphi}\right), \tag{3.49}$$

where we have used that $X = \frac{|\dot{\phi}|^2}{2}$. Taking a look at eq.(3.49) we see that the only way in which ϵ can be small is that the potential V dominates the square root. Then, performing a Taylor expansion,

$$\epsilon \simeq \frac{1}{2}\frac{G^{IJ}V_I V_J}{V^2}\cos^2\varphi \equiv \epsilon_V\,. \tag{3.50}$$

This is our multifield version of the first potential slow-roll parameter, and it is one of the main result of this thesis. It has two interesting features. The first is its connection with the single field result (3.3). In single field there is only one possible direction in field space, that is, all vectors are parallel to each other. In particular, $\cos\varphi = 1$ and we recover eq.(3.3). The second is that, due to the presence of the cosine, ϵ_V can be arbitrarily small without the usual ratio $|V'|/V$ being small. This feature is genuine to multifield inflationary models, and it turns out to be a rather deep an thought-provoking result. We will comment on it extensively at the end of this chapter.

We can also try to compute a multifield version of η_V in a similar way. Following the same steps as in single field (cf. eq.(3.4) and below), we seek a consistency relation when we ignore the acceleration term in eq.(3.42):

$$\dot{X} \simeq -\partial_t\left(\frac{V_{,K}\dot{\phi}^K}{6H}\right). \tag{3.51}$$

Then, we can plug this back into the definition of η, eq.(3.44):

$$\eta \equiv \frac{\dot{X}}{HX} \simeq \epsilon - \frac{\partial_t\left(|V'||\dot{\phi}|\cos\varphi\right)}{6H^2X}, \tag{3.52}$$

where we have used the definition of the cosine, eq.(3.48). Since $\epsilon \ll 1$, the only way in which η can be small is if the second term is small by itself. Let us compute it by systematically using eq.(3.45). We get

$$\eta \equiv \frac{\dot{X}}{XH} \simeq \epsilon + \frac{\partial_t|V'|}{H|V'|} + \frac{\partial_t\cos\varphi}{H\cos\varphi} + \frac{\dot{X}}{2XH}. \tag{3.53}$$

Thus,

$$\eta \equiv \frac{\dot{X}}{HX} \simeq 2\epsilon + 2\left(\frac{\partial_t|V'|}{H|V'|} + \frac{\partial_t\cos\varphi}{H\cos\varphi}\right), \tag{3.54}$$

so that, in close analogy to what we did in single field, it is natural to define the second term as the second potential slow-roll parameter:

$$\eta_V \equiv \frac{\partial_t|V'|}{H|V'|} + \frac{\partial_t\cos\varphi}{H\cos\varphi}. \ll 1 \tag{3.55}$$

Its interpretation is clear: neither the cosine nor the norm of the gradient of the potential should change much during one Hubble time. This second slow-roll condition has the appealing feature that, when evaluating it for the single field case we get

$$\eta_V = \frac{V''\dot{\phi}}{V'H} = -M_P^2\frac{V''}{V}, \tag{3.56}$$

where the approximated equation (3.2) has been used once more. It is immediate to see, by looking at eq.(3.6), that this is the correct result in single field. We conclude that equation (3.55) gives the correct definition for the second potential slow-roll parameter in multifield models of inflation.

3.3 Discussion

There are two major results in this chapter. On the one hand, we learnt how to understand the multifield slow-roll approximation. This was accomplished by writing the equations of motion invariant in form under an arbitrary transformation of the fields, i.e., using the covariant approach. The meaning of the second Hubble slow-roll condition, given by eq.(3.44), has now become clear: the equation of motion (3.42) suggests that the approximated equation (3.45) is the correct multifield version of the good old single field slow-roll equation of motion (1.46). It is clear by virtue of eq.(3.46) that making the acceleration of the fields small in norm is not the only way of realizing a slow-roll trajectory. Indeed, as long as the projection of the acceleration onto the velocity is small, we are safe.

On the other hand, we computed the new potential slow-roll conditions for multifield models of inflation, given by equations (3.50) and (3.55). They are the generalization of the single field parameters (3.3) and (3.6). One of their important features is that, contrary to what happened in single field, they not only depend on the potential, but also on the angle between its gradient and the velocity of the fields. These new parameters, which we believe to be correct, are in contradiction with some of the parameters seen in the literature (see, for instance, eqs.(3.11), (3.15) and (3.17)).

The two conclusions are closely related. What happened in single field was that, once in the slow-roll regime, the equation of motion reduced to the first order differential equation (1.46). Thus, once the value of the field $\phi(t)$ was known, the whole trajectory was determined. In particular, the number of efolds before the end of inflation was completely specified. When inflation is driven by multiple fields the situation is different. We learnt that neglecting the acceleration term in equation (3.33) is not the correct slow-roll approximation. In fact, $D_t\dot{\phi}^I$ does not need to be small as long as it stays orthogonal to its velocity. Then, it follows that the equation of motion in the slow-roll approximation is truly a second order differential equation. And hence, specifying the values of the fields is not enough to determine the trajectory and/or the number of efolds until inflation ends: we also need to know their velocities.

Once again, in single field the only possibility for the fields to move in the slow-roll approximation was to follow the gradient of the potential. This is best understood by noticing that the slow-roll equation of motion implies that $\dot{\phi} \propto -V'$. That is why the slow-roll parameters can be written solely in terms of the potential. Meanwhile, in multifield inflation, it doesn't necessarily follow from eq.(3.45) that the fields must follow the gradient of the potential. As a consequence, we need at least one more parameter to be able to tell if they are in a slow-roll trajectory or not. Because the term slow-roll originally comes from the idea of slowly rolling the potential hill, we like to call these trajectories that do not follow the gradient of the potential *slow-descent* trajectories.

Are slow-descent trajectories stable? Or do they decay to the usual slow-roll trajectory after a short amount of time? We studied a simple model both analytically and numerically to try to answer those questions. It is presented in the upcoming chapter.

Chapter 4

Slow-descent toy model

4.1 Introduction

In this chapter we present a toy model that serves as an example of a slow-descent trajectory. Some of the conclusions we drew in the last section will be most dramatically reaffirmed if two key points are satisfied.

First of all, we would like to proof that, driven by the same potential, two different slow-roll trajectories can be obtained by changing the initial conditions. One of them should, as usual, follow the gradient of the potential; the other, the new slow-descent trajectory, should not. That kind of setting would proof not only that slow-descent trajectories are possible, but also our claim that in multifield inflation it is not enough to specify the value of the field to determine a trajectory, we also need its velocity.

Second of all, we would be all the more delighted if such a slow-descent model could reproduce the experimental measurements of quantities such as the power spectrum or the spectral tilt. However, it should be kept in mind that our main focus is not on building a realistic model, but rather to show the validity of the general features of multifield inflation discussed in the previous section.

Having said this, let us begin to construct the slow-descent model. The main idea, as was previously commented, arises from trying to make $\dot{X}$ in eq.(3.42) small without the acceleration being small, i.e.,

$$\dot{X} = G_{IJ}\dot{\phi}^I D_t\dot{\phi}^J \simeq 0 \rightarrow \dot{\phi}^I \perp D_t\dot{\phi}^I. \tag{4.1}$$

Such a trajectory, where the velocity is perpendicular to the acceleration, is familiar to us as a circular orbit. In order to obtain a circular trajectory only two fields are necessary, and for the sake of simplicity we will only use two. In principle we could add as many fields as we wanted, but it is not expected that the basic features would change.These two fields will be called $r(t)$ and $\theta(t)$, pointing out the complete resemblance with the motion of a particle in a circular trajectory. This kind of model was introduced by I.-S. Yang in his work [23]. This chapter will revise and complete that model.

That is all we need to know to start computing. Let's go!

4.2 Analytics

We have a circular trajectory in mind. In order to describe it, we write the field space metric as the one for polar coordinates:

$$G_{IJ} = \begin{pmatrix} 1 & 0 \\ 0 & r^2 \end{pmatrix}, \tag{4.2}$$

where, as was mentioned, the fields are called $r(t)$ and $\theta(t)$.

The equation of motion for the fields are given by equation (3.41). By components they read

$$\ddot{r} - r\dot{\theta}^2 + 3H\dot{r} + V_{,r} = 0 \tag{4.3}$$

$$\ddot{\theta} + 3H\dot{\theta} + \frac{2\dot{r}\dot{\theta}}{r} + \frac{V_{,\theta}}{r^2} = 0, \tag{4.4}$$

where, for simplicity, we opted for a sum separable potential $V(r, \theta) = V(r) + V(\theta)$. The explicit form of the potential will be fixed below.

The circular trajectory is given by the following solution of these equations of motion,

$$r_{sol} \equiv R = \text{const.} \implies \dot{R} = \ddot{R} = 0 \tag{4.5}$$

$$\dot{\theta}_{sol} \equiv \dot{\theta}_0 = 0 \implies \ddot{\theta}_0 = 0. \tag{4.6}$$

Within this regime the equations of motion read

$$R\dot{\theta}_0^2 = V_{,r} \tag{4.7}$$

$$3HR^2\dot{\theta}_0 = -V_{,\theta}. \tag{4.8}$$

In order to have a solution with constant r, the force in the r axis, proportional to $V_{,r}$, must be compensated by a term that can be interpreted as a centripetal force. On the other hand, if the velocity in the θ direction is meant to be constant then we need a force (proportional to $V_{,\theta}$) that counteracts the friction $3HR^2\dot{\theta}$.

For the solution given by eqs. (4.8) and (4.7) to exist, we need the kinetic term to be positive and the two equations to be consistent with each other, this is,

$$\dot{\theta}_0^2 > 0 \implies \frac{V_{,r}}{R} > 0 \tag{4.9}$$

$$V_{,r} = \frac{V_{,\theta}^2}{3HR^2}, \tag{4.10}$$

where the second equation is obtained by equalizing $\dot{\theta}_0$ in (4.7) and (4.8).

Thus, solutions with this form always exist, provided that the conditions (4.9) and (4.10) are fulfilled. One problem, however, could be that, due to the friction to which the system is subjected, the particle would slow down and start following the gradient in the r direction. That is why we perform the following stability analysis.

Stability analysis

We suppose that the system is subjected to the trajectory given by eqs. (4.7) and (4.8), and introduce a small perturbation around those solutions, i.e., $(R, \theta_0) \to (R + \delta r, \theta_0 + \delta\theta)$. The next step is to realize that equation (4.4) can be written as

$$\partial_t \left(r^2 \dot{\theta} a^3 + V_{,\theta}\, t \right) = 0. \tag{4.11}$$

The perturbations to the Hubble parameter are slow-roll suppressed, and we can safely set $\delta H \sim \delta a$ to zero.

With this in mind, eq.(4.11) implies that at linear order

$$\delta\dot{\theta} = -\frac{2\dot{\theta}_0}{R}\delta r. \tag{4.12}$$

Now, plugging this back into the linearized version of eq. (4.3), i.e.,

$$\delta\ddot{r} - 2R\dot{\theta}_0\delta\dot{\theta} - \dot{\theta}_0^2\delta r + 3H\delta\dot{r} + V_{,rr}\delta r = 0, \tag{4.13}$$

we get a simple harmonic oscillator equation for δr:

$$\delta\ddot{r} + 3H\delta\dot{r} + (3\dot{\theta}^2 + V_{,rr}\,)\delta r = 0. \tag{4.14}$$

We can solve this equation by making the ansatz $\delta r = Ae^{i\omega t}$. For the system to be stable we need that $\omega \in \mathbb{R}$, which turns out to be the case if and only if

$$3\dot{\theta}^2 + V_{,rr} > 0. \tag{4.15}$$

Thus, this is the condition for a stable trajectory.

Slow-descent regime

We can compute the slow-roll parameters to see under what conditions a circular trajectory of this sort would be able to support inflation.

The Hubble slow-roll parameters are computed from eqs.(3.43) and (3.44), giving

$$\epsilon = \frac{9}{2}\frac{R^4 V_{,r}^2}{V_{,\theta}^2} \ll 1 \tag{4.16}$$

$$\eta \simeq 0, \tag{4.17}$$

where the two quantities have been computed for the background values (R, θ_0).

The cosine of the angle between the velocity and the gradient of the potential is

$$\cos^2\varphi = \left(1 + \frac{V_{,r}^2\,R^2}{V_{,\theta}^2}\right)^{-1}. \tag{4.18}$$

The potential slow-roll parameters of eqs. (3.50) and (3.55) give

$$\epsilon_V = \frac{V_{,\theta}^2}{2R^2V^2} \tag{4.19}$$
$$\eta_V = \frac{V_{,\theta\theta}}{R^2\left(R\frac{V_{,r}}{2} + V\right)}. \tag{4.20}$$

To make later results sharper, we can also explicitly compute the first potential slow-roll condition that is frequently used in the literature, here given by eq. (3.11):

$$\begin{aligned} \epsilon_V^{sr} &= \frac{1}{2}\frac{V_{,\theta}^2 + R^2V_{,r}^2}{R^2V^2} \\ &= \epsilon_V + \frac{1}{2}\left(\frac{V_{,r}}{V}\right)^2, \end{aligned} \tag{4.21}$$

where the label *sr* indicates that this expression is only valid on the usual slow-roll approximation, but not in the slow-descent regime we are investigating. It is interesting to see how it can be written down in terms of what we consider to be the adequate parameter, ϵ_V. Clearly, if $V_{,r} > V$ then $\epsilon_V^{sr} > \epsilon_V$ and will not be a good quantity to parametrize inflation.

The slow-descent regime we want to build requires both $\epsilon \ll 1$ and $\cos\varphi \ll 1$. Note that imposing the cosine of φ to be small is equivalent to asking that the gradient of the potential goes in the r direction, i.e.,

$$\cos\varphi \ll 1 \implies RV_{,r} \gg V_{,\theta}\,. \tag{4.22}$$

Combining the two conditions in one line:

$$\sqrt{\frac{9}{2}}R^2V_{,r} \ll V_{,\theta} \ll RV_{,r}\,. \tag{4.23}$$

It is now time to choose a potential. It turns out, as will become clear soon, that a potential as simple as

$$V(r,\theta) = \frac{1}{2}m^2r^2 + c\sqrt{b^2+\theta^2} \tag{4.24}$$

can, for certain values of the parameters m^2, c and b, drive a slow-descent trajectory. Although it may seem strange at first, the θ dependence of the potential is quite simple and easy to understand. In the limit where θ is large it becomes linear $V(\theta) \simeq c\theta$. On the other hand, when θ is small, $V(\theta) \simeq cb$, which is a cosmological constant. This is a choice that ensures linear behavior in a region of our interest, and at the same time no singularity at the origin (that would appear if we had written down the simpler $V(\theta) = c\theta$). It is also important to notice that in our simulations θ does not run from 0 to 2π, but rather $\theta \in \mathbb{R}$.

With this potential, the conditions (4.23) read, in the region where $b \ll \theta$.

$$\sqrt{\frac{9}{2}}m^2R^3 \ll c \ll m^2R^2, \tag{4.25}$$

which can be satisfied for certain values of m^2, c and R, as will be clear below.

We gathered enough analytic information to properly understand the simulations. The next section presents our results.

4.3 Numerics

Before doing anything else, it is wise to use the number of efolds N as the time variable to express the equations of motion we want to solve, eqs. (4.3) and (4.27). They become

$$r'' + \epsilon r' - r\theta'^2 - 3r' + \frac{V_{,r}}{H^2} = 0 \tag{4.26}$$

$$\theta'' + \epsilon\theta' - 3\theta' + \frac{2r'\theta'}{r} + \frac{V_{,\theta}}{r^2 H^2} = 0, \tag{4.27}$$

where the primes denote derivatives with respect to the number of efolds, and the convention in which the number of efolds decreases has been used, i.e., $dN = -Hdt$. As we know inflation has to last about 60 efolds the choice of writing the equations of motion in terms of N is a wise one: inflation simply starts around $N = 60$ and ends at $N = 0$.

We evaluated the full equations of motion (4.3) and (4.4) with the following initial conditions and values of the parameters:

- **Initial conditions**

$$\begin{aligned} r(60) &= 6.7 \times 10^{-5} M_P \\ r'(60) &= 1.9 \times 10^{-7} M_P \\ \theta(60) &= -1.4 \times 10^{5} \\ \theta'(60) &= 1.6 \times 10^{3} \end{aligned}$$

- **Parameters**

$$\begin{aligned} m^2 &= 5 \times 10^{-4} M_P \\ c \ &= 1.8 \times 10^{-14} \\ b^2 &= 10^{3} \end{aligned}$$

A handful of things may be noted about these choices.[1] First of all, notice that the field r has sub-Planck values. The same happens with the cosmological constant $\sim cb$. One can check that all the conditions derived above are satisfied. Most importantly, this values lay in a regime where eqs. (4.15) and (4.25) are satisfied.

Figure 4.1 shows the circular trajectory that was expected in the $(x, y) \equiv (r\cos\theta, r\sin\theta)$ plane. The particle moves slower in the beginning of inflation (red line) than in the end (blue line). Also, notice that the radius r increases during inflation. The cause of both things is that the field is rolling down the potential in the $V_{,\theta}$ direction, and so $\dot{\theta}$ is becoming bigger as time goes by. The larger $\dot{\theta}$ is, the larger r needs to be to maintain a stable circular orbit.

Another way of parametrizing that the trajectory the fields follow is the one that we expected to be is to check whether $\cos\varphi$, as defined in eq.(3.48) is small. As Figure 4.2 shows, this is indeed the case.

[1] Our actual computation began with different initial conditions, thousands of efolds before the condition $\epsilon = 1$ was reached. All the discussion in this section, including the values mentioned, correspond to 60 efolds before inflation ended.

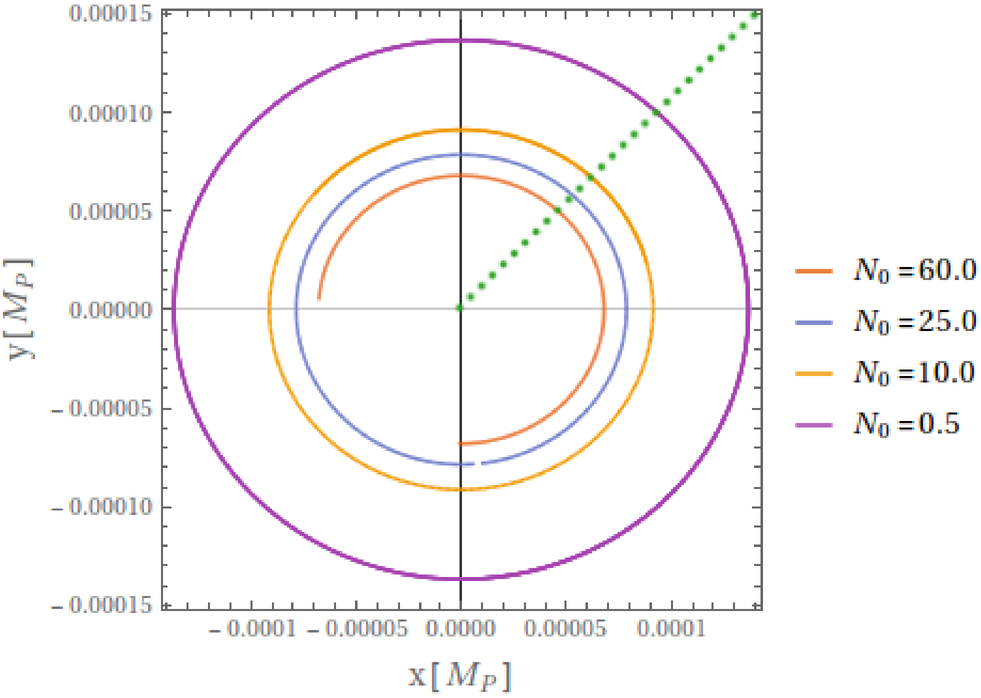

FIGURE 4.1: Circular trajectory of the particle at different stages of inflation. The fields x and y are defined as the usual Cartesian coordinates: $(x, y) \equiv (r\cos\theta, r\sin\theta)$. The legend shows the initial number of efolds of the lines, and all of them correspond to 0.003 efolds. The dotted green line shows to a usual slow-roll trajectory, where the fields simply follow the gradient of the potential.

We can conclude that the particle stays in an almost perfect circular orbit, whose radius is increasing slowly.

The Hubble and the potential slow-roll parameters are shown in Figure 4.4. This is perhaps the most important plot of this section. It shows how the new potential slow-roll conditions ϵ_V and η_V, that were derived above, stay small in this new paradigm of slow-descent inflationary trajectories.

On the other hand, we plotted the incorrect potential slow-roll parameter ϵ_V^{sr}, defined in eq. (3.11). As we can see in Figure 4.5, it is obviously not the proper parameter to judge whether an inflationary trajectory will happen or not.

Last but not least, we computed the scalar power spectrum using the naive single field result of eq. (2.94), and it is shown in Figure 4.6. One should not take this result too seriously; it is only useful as a rough estimate of the normalization of the power spectrum.

4.4 Discussion

Several conclusions can be drawn from these results.

First of all, we have shown that a stable inflationary trajectory that does not follow the gradient of the potentials exists. This is already quite remarkable, as these kind of trajectories are never considered in the standard literature we have come across. Even more, we did so employing a potential that clearly accepts usual slow-roll trajectories. This points towards the direction of what we concluded in the previous section: to unambiguously characterize a multifield inflationary trajectory we need

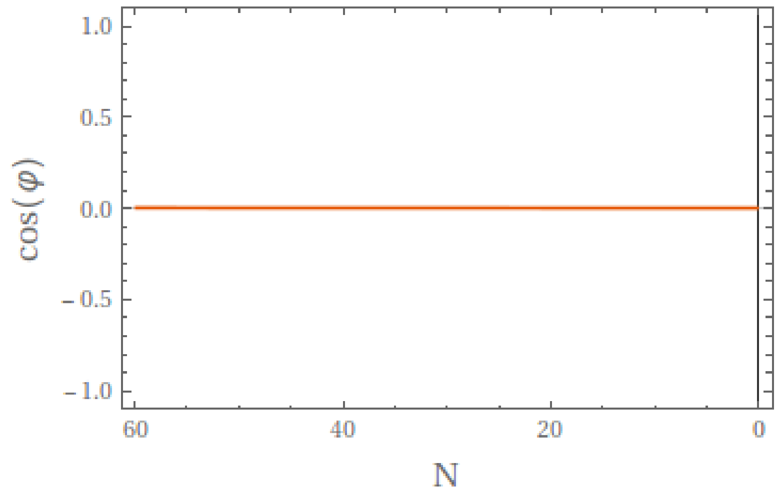

FIGURE 4.2: The cosine of the angle between the gradient of the potential $\nabla V \simeq V_{,r}\hat{u}_r$ and the velocity of the fields $\dot{\phi}^I \simeq -r\dot{\theta}\hat{u}_\theta$, where $\hat{u}_r$ and $\hat{u}_\theta$ are unit vectors in the directions of r and θ, respectively.

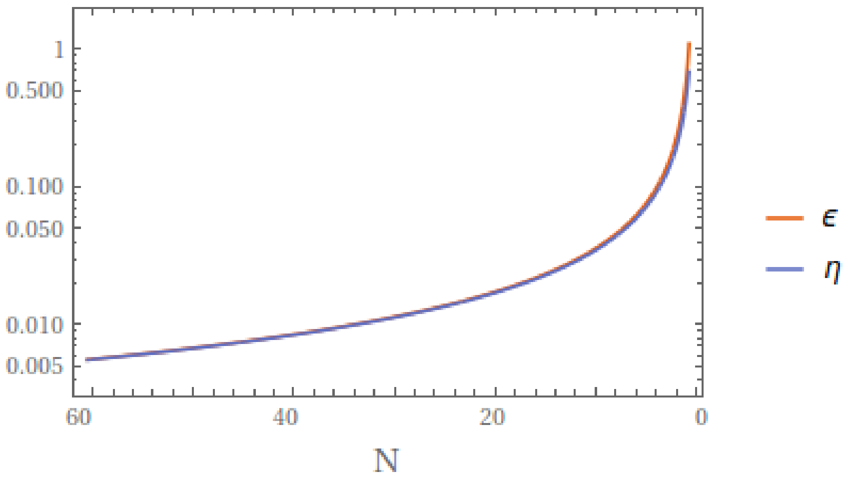

FIGURE 4.3: The Hubble slow-roll parameters ϵ and η.

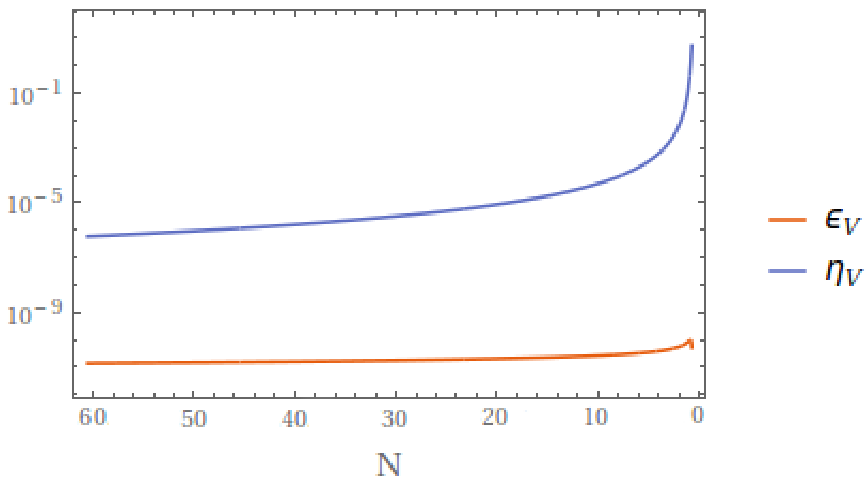

FIGURE 4.4: Hubble and potential slow-roll parameters. It is aparent how the potential slow-descent parameters stay small until inflation ends $\epsilon = 1$.

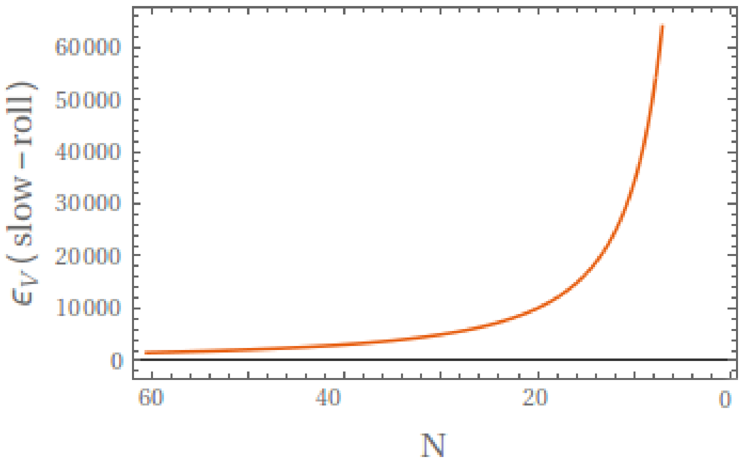

FIGURE 4.5: The incorrect parameter ϵ_V^{sr}. If we were only paying attention to this parameter, we would never say that this plot corresponds to an inflationary trajectory, as ϵ_V is bigger than 1 the whole time.

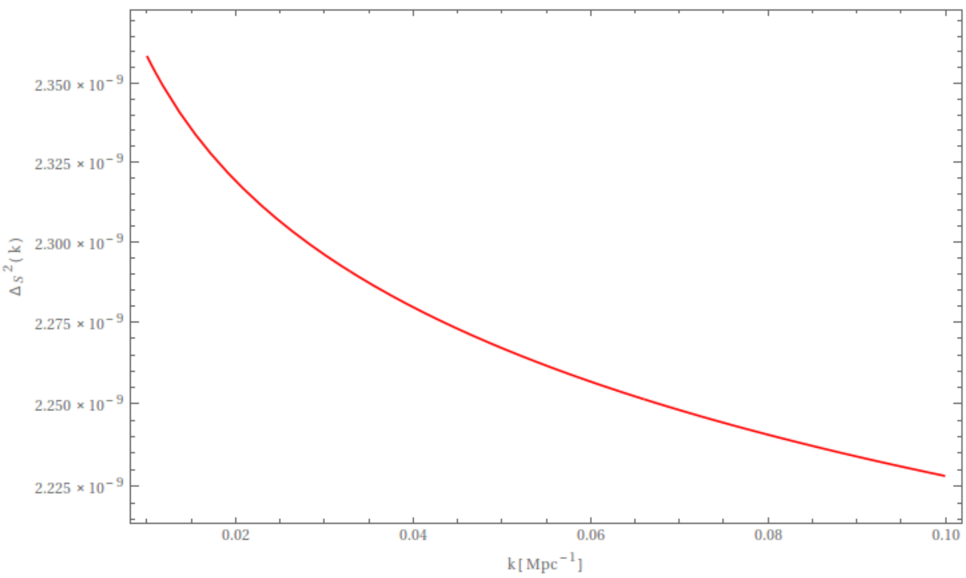

FIGURE 4.6: Matter power spectrum, $\Delta_s^2(k)$, for our toy model. We can see that it loosely fits the experimental value of $\Delta_s^2(k = 0.05Mpc) \simeq 2.2 \times 10^{-9}$ measured by Planck [1].

to specify both the value of the field and its velocity at some given time. This is, as was mentioned above, one of the main results of the present work.

Nevertheless, our toy model did present an inconvenience to this respect. The dotted green line of Figure 4.1 is not exactly an inflationary trajectory in the sense that the usual slow-roll trajectories end inflation at larger values of the r field, this is, higher in the potential. Therefore, we did not find two intersecting inflationary trajectories. Although it may sound like it, it is not a major drawback; we can simply argue that either two intersecting inflationary trajectories might exist for other values of the parameters and for a different set of initial conditions, or that our potential was too naive (which certainly was) and that in more complex models, which could include more fields, trajectories could cross one another. That is our opinion: there must be multifield models in which the usual slow-roll and the new slow-descent inflationary trajectories intersect each other.

Another relevant conclusion is that for slow-descent trajectories the right potential slow-roll parameters were the ones we derived in section 3.2.2. We also saw that the parameters proposed until now in the literature lead to the wrong conclusions about the inflationary nature of the trajectories. Indeed, if the parameter ϵ_V^{sr} of eq. (3.11) (which in this particular model is given by eq. (4.19)) was the correct one to decide whether a given trajectory inflates or not, then its values in Figure 4.5 should be smaller than one.

As a last remark, the power spectrum of Figure 4.6 should not be taken too seriously. Instead of computing the fluctuations of the two fields, we simply used the single field expression (2.94). Thus, its interest (if it has any) is that the normalization of the power spectrum loosely coincides with the experimental measurement (cf.equation (2.72)). Although this model was a toy model without further pretensions than to demonstrate that the ideas developed above were not mere speculations, the normalization of the power spectrum is acceptable. This fact does nothing but support the idea that these kind of slow-descent inflationary trajectories are not only mathematically possible, but probably also *physical*.

Outlook and further research

Several partial results were obtained in the present work. The most direct and obvious one is the correct interpretation of the multifield slow-roll conditions, determined in eq. (3.45). With that improved understanding, two concrete features were discovered. On the one hand, the correct multifield potential slow-roll parameters were found, as shown in eqs. (3.50) and (3.55). These do not depend only on the potential anymore, but are also a function of another parameter: the angle φ between the velocity of the fields and the gradient of the potential. On the other hand, we realized that a new kind of slow-roll trajectory, the *slow-descent* trajectory, was possible. These kind of trajectories do not follow the gradient of the potential, as is the case in the usual slow-roll scenario. The two ideas are closely related, since the angle φ is necessary to parametrize the smallness of ϵ_V and η_V in slow-descent models of inflation.

These points are most dramatically strengthened by the toy model that was presented in Chapter 4. Figure 4.1 shows the two possible trajectories for the fields, and by comparing Figures **??** and 4.5 it can be concluded that the potential slow-roll parameters introduced do a much better work. Moreover, we showed that this example realized a stable slow-descent trajectory.

There was another interesting result, discussed in section 2.5, that was less highlighted because it fell outside the main scope of the thesis. By considering multifield models that did evolve along the traditional slow-roll trajectories, equation (2.136) was obtained. The angle between the gradient of the number of efolds and the velocity of the fields, α, can be interpreted as the quantity that parametrizes the presence of more than one field. In fact, $\alpha = 0$ reduces to the single field consistency relation (2.135), whereas $\alpha \neq 0$ is only possible if more dimensions are available in field space. The interest of this result resides in its potential measurability in the near future. Improved experimental constraints on the tensor to scalar ratio r and the tensorial tilt n_t could therefore disprove or validate single field models of inflation.

Harkening back to the main theme of this thesis, there are some more speculative and far reaching ideas that suggest the direction towards which further research could point. When the δN formalism was introduced in section 2.4, one of the assumptions we made was that eq.(2.122) was a good approximation of the trajectory of the fields. Using that equation, we were able to write the number of efolds, which is in principle a function of both the values and the velocities of the fields, as a function of the fields only, this is, $N(\phi^I, \dot{\phi}^I) = N(\phi^I)$. But we have seen that this is not the most general slow-roll approximation, and one should be more careful when making that assumption. In fact, we showed that two inflationary trajectories can intersect in multifield inflation (see, once again, 4.1, i.e., two trajectories can have different $\dot{\phi}^I$ for the same ϕ^I. One of the future tasks to complete this work would be to extend the δN formalism, a crucial tool to compute the power spectra in multifield models, to the most generic slow-roll conditions described here.

There is another direction in which further research could go. Our slow-roll parameter ϵ_V indicates that provided $\cos\varphi^2 \ll 1$, inflation can happen for any shape of the potential. If such a condition was naturally realized in multifield inflation for a large class of potentials, it could be an argument in favor of these kind of models: the likelihood of our universe having undergone an inflationary phase would be greater in the case of multifield models, where inflation could happen for any potential, than in the single field one, where the potential has to have a concrete shape in order to inflate. In order to gain some analytic insight, we compute in Appendix B the average of the square of the cosine between two random vectors in N dimensions. The result, given in eq. (B.6) is stimulating. It insinuates that $\langle\cos^2\varphi\rangle = 1/N$ and therefore ϵ_V can be made arbitrarily small simply by adding fields.

It goes without saying that ϕ^I and $V^{,I}$ are not random vectors, but rather quantities that are determined by some equations of motion. Hence, the naive result of Appendix B does not directly apply here. Anyway, it would be interesting to evaluate that quantity more realistically. The only way we can think of is using numerical methods together with an effective implementation of random potentials to solve the full equations of motion.

The primordial question that motivated us to do this work, whether inflation was driven by a single or by many scalar fields, is, sadly enough, unanswered yet. Nevertheless, it is comforting to think that we have taken some small steps in what hopefully is the right direction. Although, giving it a second thought, perhaps it is not so sad. Knowing the answer to those kind of questions would prevent us from giving our best to solve the conundrum, which is, after all, the physicist's most natural state.

THE END

Appendix A

Multifield slow-roll consistency relation

In this short appendix we compute the relation between the tensor to scalar ratio and the tensorial tilt for multifield slow-roll models of inflation.

The power spectrum for the tensorial perturbations and its tilt are still given by eqs. (2.97) and (2.107) in multifield inflation, as introducing more scalar degrees of freedom does not affect the tensorial part of the equations (remember the SVT decomposition!). Now, to compute the tensor to scalar ratio r we can use equation (2.129) to see that

$$r \equiv \frac{\Delta_t^2}{\Delta_s^2} = \frac{8}{N_{,I}N_{,J}G^{IJ}}, \tag{A.1}$$

with summation over indices understood.[1] The quantity in the denominator is the norm of the gradient of the number of efolds squared. We can rewrite eq. (A.1) as

$$r = \frac{8}{|N'|^2}. \tag{A.2}$$

Moving on, the following relation will be useful

$$H \equiv \frac{dN}{dt} = \frac{\partial N}{\partial \phi^I}\frac{\partial \phi^I}{\partial t} = |N'||\dot{\phi}|\cos\alpha, \tag{A.3}$$

where we have used the definition of the number of efolds $dN \equiv H dt$, and we have introduced α, the angle between the gradient of the number of efolds and the velocity of the fields. Using equation (A.3), we can rewrite equation (A.2) as follows:

$$r = \frac{8|\dot{\phi}|^2\cos^2\alpha}{H^2} = 16\epsilon\cos^2\alpha, \tag{A.4}$$

where equation (3.35) has been used to write it in terms of ϵ.

Despite its simplicity, it is a rather interesting result that has not, as far as we know, been computed in the literature before. In one line, it states that in multifield slow-roll there is an analogous consistency relation to that of single field inflation, derived in eq.(2.108), and it is given by

[1] For the readers that are coming here directly from Chapter 2, it should be noted that multifield models with non-trivial field space metric G^{IJ} are introduced in Chapter 3.

$$r = -8n_t \cos^2 \alpha. \tag{A.5}$$

Its implications are discussed in the closure of Chapter 2.

Appendix B

$\langle \cos^2 \varphi \rangle$ between two random vectors in N dimensions

In this appendix we compute the average of the cosine squared of an angle between two random vectors in N dimensions. As a warm up, let us perform the calculations in 3 dimensions. We can always fix one of the vectors to point in the zenith direction, so that the angle between this one and the other will be given by the inclination φ.

We first want to compute the probability density function. The area element of the unit sphere is $\sin\varphi\, d\varphi\, d\theta$. To turn this into a probability density function we have to divide it by the total area of the unit radius sphere (the vectors are unitary), this is, 4π. The probability density function then is

$$f(\varphi) = \frac{1}{4\pi}\int_0^{2\pi} \sin\varphi d\theta = \frac{1}{2}\sin\varphi. \tag{B.1}$$

We can check that this is indeed a well defined probability density function by noting that

$$\int_0^{\pi} f(\varphi) d\varphi = 1. \tag{B.2}$$

Let us now generalize this computation to N dimensions. The perimeter of a circle of radius $\sin\theta$ is

$$\int_0^{2\pi} \sin\varphi d\theta. \tag{B.3}$$

In order to obtain an expression analogous to (B.1) in N dimensions, we should take the surface of an $N-2$ sphere of radius $\sin\varphi$ and divide it by the surface of a $N-1$ sphere. We get

$$f(\varphi) = \frac{S_{N-2}}{S_{N-1}}\sin^{N-2}\varphi = \pi^{-1/2}\frac{\Gamma\left(\frac{N}{2}\right)}{\Gamma\left(\frac{N-1}{2}\right)}\sin^{N-2}\varphi. \tag{B.4}$$

Once the probability density function is computed, calculating the following quantities does not require too much work:

$$\langle\cos\varphi\rangle = \int_0^{\pi}\cos\varphi f(\varphi) d\varphi = \frac{\pi^{-1/2}}{n-1}\frac{\Gamma\left(\frac{N}{2}\right)}{\Gamma\left(\frac{N-1}{2}\right)}\sin^{N-1}\varphi\Big|_0^{\pi} = 0 \tag{B.5}$$

$$\left\langle\cos^2\varphi\right\rangle = \int_0^\pi \cos^2\varphi f(\varphi)d\varphi = \pi^{-1/2}\frac{\Gamma\left(\frac{N}{2}\right)}{\Gamma\left(\frac{N-1}{2}\right)}\frac{\pi^{1/2}\Gamma\left(\frac{N-1}{2}\right)}{2\Gamma\left(\frac{N}{2}+1\right)} = \frac{1}{N}. \tag{B.6}$$

This computation will become useful when discussing possible values of the new slow-roll parameter ϵ_V. (See conclusion chapter).

Acknowledgements

I am very grateful to Enrico Pajer for giving me the opportunity to experience what research is like under such a privileged supervision. Grazie mille!

On a similar note, many thanks to Víctor for being the other half (the pessimistic half, but also the half doing the most reliable computations) of this thesis. Moltes gràcies, exconvíctor!

I won't forget about Ezequiel, who didn't help at all with the thesis, but did with everything else. Gracias, bicho! Vos sos B.I.G!

Thanks a lot to the awesome group of students that have walked these two years' winding road with me. Everything was much easier with your friendliness. Dank jullie wel!

I am also grateful, though in another language, to the following people:

Al aita y a la ama, por todo. Pero sobre todo por sus valiosísimas revisiones del texto, con certeros comentarios estilísticos sobre el idioma, y por supervisar que durante todo el proceso mi organismo dispusiera de los nutrientes necesarios. A la amona, por esas revelaciones sobre qué pasó al principio de los tiempos. A mis amigos de Irun (sobre todo a los que me han venido a visitar. A los demás, ahora que lo pienso, no), y en especial a aquellos a los que Imanol mentó en su tesis, porque si no los menciono ahora se van a poner celosos. Físicos experimentales, todos ellos: Eneko, experto en física acústica aplicada; Ander, topólogo Euclideano realista; y Xabi, el Dumbledore de los Feynman diagrams. Al propio Imanol todavía no sé si agradecerle o desagradecerle nada, al ser, al menos en parte, culpa suya que yo tomara este camino.

Anttoni, lan hau txikitako problema horien bertsio heldua baino ez delako. Azkenik, eta bihotz-bihotzez, Maku, Ibai eta Urkiri, beharrean zeudenak beraiek zirenean bere bizi-gogoa besteekin partekatzeagatik.

Bibliography

[1] Planck Collaboration. “Planck 2013 results. XVI. Cosmological parameters”. In: *arXiv.org* 1303 (2013), p. 5076. arXiv: 1303.5076.

[2] Daniel Baumann. “Part III Mathematical Tripos 10 -34”. In: ().

[3] E Hubble. “a Relation Between Distance and Radial Velocity Among Extra-Galactic Nebulae.” In: *Proceedings of the National Academy of Sciences of the United States of America* 15.3 (1929), pp. 168–173.

[4] Arno A. Penzias and Robert Woodrow Wilson. “A Measurement of excess antenna temperature at 4080-Mc/s”. In: *Astrophysical Journal* 142.9 (1965), pp. 419–421. arXiv: arXiv:1011.1669v3.

[5] A. A. Starobinskii. *Spectrum of relict gravitational radiation and the early state of the universe.* 1979.

[6] Alan H. Guth. “Inflationary universe: A possible solution to the horizon and flatness problems”. In: *Physical Review D* 23.2 (1981), pp. 347–356.

[7] A. D. Linde. “Coleman-Weinberg theory and the new inflationary universe scenario”. In: *Physics Letters B* 114.6 (1982), pp. 431–435. arXiv: arXiv:1011.1669v3.

[8] Andreas Albrecht and Paul J. Steinhardt. “Cosmology for grand unified theories with radiatively induced symmetry breaking”. In: *Physical Review Letters* 48.17 (1982), pp. 1220–1223.

[9] Scott Doldelson. *Modern Cosmology.* Elsevier, 2010.

[10] Steven Weinberg. *Cosmology.* Oxford University Press, 2008.

[11] Daniel Baumann. “TASI Lectures on Inflation”. In: (2009). arXiv: 0907.5424.

[12] D. Langlois. “Inflation and cosmological perturbations”. In: *Lecture Notes in Physics* 800 (2010), pp. 1–57. arXiv: 0306275 [astro-ph].

[13] Juan Maldacena. “Non-Gaussian features of primordial fluctuations in single field inflationary models”. In: *Journal of High Energy Physics* 05.05 (2003), pp. 013–013. arXiv: 0210603 [astro-ph].

[14] D. S. Salopek and J. R. Bond. “Nonlinear evolution of long-wavelength metric fluctuations in inflationary models”. In: *Physical Review D* 42.12 (1990), pp. 3936–3962.

[15] Karim A. Malik and David Wands. “Evolution of second-order cosmological perturbationsMalik, K. A., & Wands, D. (2004). Evolution of second-order cosmological perturbations. Journal of Cosmology and Astroparticle Physics, 2004(01), 003–003. http://doi.org/10.1088/1475-7516/2004/01/003”. In: *Journal of Cosmology and Astroparticle Physics* 2004.01 (2004), pp. 003–003. arXiv: 0307055 [astro-ph].

[16] Steven Weinberg. “Adiabatic modes in cosmology”. In: *Physical Review D* 67.12 (2003). arXiv: 0302326 [astro-ph].

[17] David Lyth and Yeinzon Rodríguez. “Non-Gaussianity from the second-order cosmological perturbation”. In: *Physical Review D* 71.12 (2005), p. 123508. arXiv: 0502578 [astro-ph].

[18] Naonori S Sugiyama, Eiichiro Komatsu, and Toshifumi Futamase. “{{}\delta{}}N formalism”. In: (2012). arXiv: 1208.1073.

[19] P. a. R. Ade et al. “Planck 2015 results. XX. Constraints on inflation”. In: *Astronomy & Astrophysics* 571 (2015), A22. arXiv: 1303.5082.

[20] Misao Sasaki and Ewan D. Stewart. "A General Analytic Formula for the Spectral Index of the Density Perturbations produced during Inflation". In: *Progress of Theoretical Physics* 95.1 (1995), p. 10. arXiv: 9507001 [astro-ph].

[21] Filippo Vernizzi and David Wands. "Non-Gaussianities in two-field inflation". In: *Journal of Cosmology and Astroparticle Physics* 2006.05 (2006), pp. 019–019. arXiv: 0603799 [astro-ph].

[22] Richard Arnowitt, Stanley Deser, and Charles W. Misner. "The Dynamics of General Relativity". In: *General Relativity and Gravitation* 40.9 (2004), pp. 1997–2027. arXiv: 0405109 [gr-qc].

[23] I-Sheng Yang. "The Strong Multifield Slowroll Condition and Spiral Inflation". In: *Phys.Rev.* D85 (2012), p. 123532. arXiv: 1202.3388 [hep-th].

[24] David Langlois and Sébastien Renaux-Petel. "Perturbations in generalized multi-field inflation". In: *Journal of Cosmology and Astroparticle Physics* 2008.04 (2008), p. 17. arXiv: 0801.1085.